Multiobjective and Simultaneous Two-Problem Allocation of a Hybrid Solar-Wind Energy System Joint with Battery Storage Incorporating Losses and Power Quality Indices

Hindawi
International Journal of Energy Research
Volume 2023, Article ID 6681528, 24 pages
https://doi.org/10.1155/2023/6681528

Research Article

Multiobjective and Simultaneous Two-Problem Allocation of a Hybrid Solar-Wind Energy System Joint with Battery Storage Incorporating Losses and Power Quality Indices

Mohammad Jafar Hadidian Moghaddam,[1] **Mohammad Bayat**,[1] **Amin Mirzaei**,[1] **Saber Arabi Nowdeh**,[2] **and Akhtar Kalam**[3]

[1]*Department of Electrical Engineering, Faculty of Engineering, Arak University, Arak 38156-8-8349, Iran*
[2]*Technical and Vocational Training Center, Gorgan, Golestan, Iran*
[3]*College of Engineering and Science, Victoria University, Melbourne, Australia*

Correspondence should be addressed to Saber Arabi Nowdeh; saber.arabi17@gmail.com

Received 20 July 2023; Revised 29 September 2023; Accepted 13 October 2023; Published 15 November 2023

Academic Editor: Subhashree Choudhury

In this paper, a multiobjective and simultaneous two-problem allocation of a hybrid distributed generation (HDG) system comprises of solar panels, wind turbines, and battery storage is proposed in a 33-bus unbalanced distribution network which can decrease total losses and improve power quality (PQ). The PQ indices are defined as voltage swell, total harmonic distortion, voltage sag, and voltage unbalance. In this study, the two problems of hybrid system design and its allocation in the distribution network are solved simultaneously. In the allocation problem, the HDG is placed ideally in the network to reduce energy losses and enhance PQ indices. The HDG is measured to minimize the cost of energy generation, including the initial investment, maintenance, and operation costs. The decision variable including the size of HDG components and its location is optimally determined via escaping bird search (EBS) algorithm which is inspired by the maneuvers of the swift bird to avoid predation. The results cleared that the proposed methodology using the wind and solar resources integrated with battery storage reduced the losses, voltage swell, total harmonic distortion, voltage sag, and voltage unbalance by 34.31%, 49.60%, 0.25%, 40.19%, and 2.18%, respectively, than the base network via the EBS and the results demonstrated the better network performance using all renewable resources against wind or solar application only. The outcomes demonstrated the superiority of the EBS in achieving the highest improvement of the different objectives compared with particle swarm optimization (PSO) and manta ray foraging optimization (MRFO). Moreover, the superior capability of the EBS-based methodology is proved in comparison with previous studies.

1. Introduction

1.1. Motivation. Due to many reasons such as the rising trend in electrical energy consumption, the high manufacturing and start-up costs of large-scale power plants, and greenhouse gases caused by burning fossil fuels for power generation, utilities are increasingly turning to the construction of small-scale power plants [1]. These low-cost, near-end-user network resources need little upfront investment and may be up and running quickly. Furthermore, they provide pollutant-free or low-polluting electricity [2, 3]. It is possible to increase demand by using clean and efficient renewable energy resources (RESs). Therefore, solar and wind energy-based (i.e., solar panel (SP) and wind turbine (WT)) systems are termed DGs. Apart from the stated benefits, DGs can also reduce power losses, sell active/reactive power, and enhance the power quality (PQ) and voltage profile in distribution networks when used properly [4]. DG sources must be situated adequately. Without adequate DG capacities and proper locations, the network will operate worse than before. Moreover, this condition will also have negative impacts on the network's losses and PQ indices. As a result, one of the most critical

considerations in the installation and operation of DGs is their right size and location. SP and WT locations and sizes are often done for a variety of reasons, including loss decrement, reliability enhancement, and voltage profile improvement [5, 6]. On the other hand, metaheuristic methods can be used to determine the optimal installation location and resource capacity of the DGs. In recent years, the use of these methods has been widely welcomed to achieve the optimal solution to obtain the best characteristics of the distribution networks [7, 8].

1.2. Literature Review. As off-grid storage mechanisms are explored in this part, literature studies are carried out on the optimization [7, 8] of hybrid distributed generation (HDG) systems with grid-connected storage mechanisms and HDG system design. A nontraditional multiobjective PSO is suggested in [9] to discover the optimal location and size of DGs. After installation, cost analysis and power losses are considered in this paper. Siting and sizing of DGs by PSO and genetic algorithm (GA) are done in [10]. Some important objectives such as power losses, load shedding, and voltage deviations are minimized by the proposed techniques. Improved simulated annealing PSO (ISA-PSO) proposed in [11] as an efficient algorithm is applied to determine the capacity and location of DGs. Total costs, including operation, electricity, pollution, and grid losses, are considered in the paper. Moreover, constraints comprise bus voltage, power flow, capacity, and conductor current. Total energy cost, average voltage drops, and power losses can be minimized by using the artificial bee colony (ABC) algorithm, which is proposed in [12]. An artificial hummingbird algorithm (AHA) is applied to consider the capacity and placement of WTs and SPs in [13] for a multiobjective function. The optimization challenge is aimed at minimizing total emissions, costs, voltage stability, and voltage deviation. It is possible to locate and size the DGs most efficiently by using hybrid genetic PSO as mentioned in [14]. Consequently, total power losses and voltage regulations will be improved. The paper in [15] describes an ant lion optimizer algorithm- (ALOA-) based method for optimizing the size and location of SPs and WTs in the network to decrease losses and increase voltage stability.

Although most SP and WT systems in the grid do not employ HDG and additionally include battery storage systems (SWBHDG), they are deployed as wind-only systems or in conjunction with SPs. A multiobjective optimization procedure is proposed in [16] to support the planning of SWBHDG. The objectives of the research include expanded energy production density, levelized energy cost, and net present value. Among other sources in SWBHDG, WTs produced flicker, which decreases power quality significantly in distribution networks. A crow search algorithm (CSA) with a differential operator is proposed in [17] to minimize active and reactive losses, flicker emission, voltage deviation, and battery storage (BS) system cost. Using a combination of modified perturb and observe (MP&O) and modified flower pollination algorithms (MFPA) is used in a SWBHDG to minimize overall cost and total harmonic distortion (THD) and to achieve stable power [18]. Considering reliability limits and seasonal changes, [19] developed an off-grid SWBHDG system to minimize yearly costs. The paper in [20] employs a renewable hybrid system's technical-economic design to reduce current value costs in Malaysia. The paper in [21] shows how to use HOMER software to reduce the current value cost of energy production in an off-grid SWBHDG system with a diesel generator for remote places. Employing the artificial electric field algorithm (AEFA) which is proposed in [22] presents an optimum SWBHDG system design as a multiobjective function to reduce the cost of system lifespan containing the cost of purchasing power, the cost of components, and the cost of CO_2 emissions. Using the improved harmony search algorithm (IHSA) to maximize network load supply and reduce system yearly costs, [23] demonstrates the SWBHDG system's capabilities. The key target of [24] is to calculate the economic feasibility of SWBHDG in the Brazilian electric system. The analysis is done by changing different variables such as installation cost, battery bank investment, and discount rate based on three scenarios. The paper in [25] constructs an optimum SWBHDG system using the big bang algorithm (BBA). Consideration of dependability restrictions minimizes original investment expenses as well as replacement costs and maintenance. The SWBHDG system is designed optimally in [26] by applying new improved moth flame optimization (IMFO) to decrease system costs along with the loss of load and CO_2 emission cost under consideration of reliability. According to [27], optimization of the SWBHDG system uses the grey wolf optimizer (GWO) method to reduce yearly system costs related to power balance constraints. The paper in [28] suggests utilizing the perturb and observe (P&O) controller applied for maximum power point tracking (MPPT) to optimize the SWBHDG to decrease costs and create high power quality output. As shown by [29], a SWHDG system may be designed with or without BS to accommodate a variety of system configurations using varying solar and wind resource capabilities to apply in hot climates. HOMER software is used by [30] to develop a grid-connected SWHDG system that meets household load demand while also minimizing energy expenses. According to the data, the energy system described is not cost-effective even at interest rates of up to 80%. A grid-connected and off-grid SWHDG system with a FC is designed optimally by utilizing the imperialist competitive algorithm (ICA) and taking the marketability of the power into account to reduce energy generating costs and the unsupported energy cost of system demand. The optimal location and size of WT, SP, and FC in the system are achieved by using the PSO algorithm. Moreover, the results show that gas emissions are reduced significantly [31].

In previous years, different studies [32–39] were conducted to determine the effects of using SP and WT systems on the characteristics of the distribution network. In [33], a multiobjective approach is suggested for sizing a grid-connected system composed of WT and SP. Reducing emissions and life cycle costs are the key objectives. A set of Pareto-optimal solutions are generated using the suggested model. Fathi et al. [34] offer a novel approach known as information gap decision theory (IGDT) for lowering losses and expenses while boosting system dependability. The application of the optimization method is made to a renewable system made up of SP and WT. A hybrid system made

up of PV, WT, and BS is used with the metaheuristic improved whale optimizer algorithm (IWOA) to reduce active losses and voltage variations [35]. In [37], the allocation of losses is carried out using a current summation procedure. In a network with radial distribution with DG, this technique is taken into account. The size and location of DGs, electric cars, and shunt capacitors are all optimized in [40] using the grasshopper optimization algorithm (GOA). By analysing demand response and time-varying voltage-dependent load models, a novel method is presented in [41] to choose the capacity and location of DGs. Spring search algorithm (SSA) is used in [42] to optimize the size and location of capacitor banks and DGs. In [43], the sine cosine algorithm (SCA) is used to optimize the distribution of DGs. In [44], the design of a hybrid system made up of a diesel/WT/SP/BS is optimized using PSO and the constraint method. On balanced distribution networks, the majority of the aforementioned techniques are evaluated for efficiency. In [45], network reconfiguration is done using adaptive ant colony optimization (AACO) to reduce power losses. The efficiency of the suggested technique is tested on both balanced and unbalanced distribution networks. In order to reduce power losses and improve system performance, such as total harmonic voltage distortion, annual cost, voltage imbalance factor, and voltage profile, [46] uses a fuzzy-genetic algorithm (FGA). Testing on an imbalanced 33-bus distribution system shows that the proposed solution is preferable. In [47], a modified heuristic algorithm (MHA) is suggested to reduce damage as well as costs caused by power outages. On both balanced and unbalanced networks, the suggested technique is evaluated.

1.3. Research Gap. There is more research on the best use of DG or HDG resources in the distribution network to minimize losses and increase voltage stability and voltage profile, but their impact on the PQ indices is not fully studied. Most research has also focused on balanced distribution networks, which does not make sense given the imbalance nature in the network phases. Although off-grid HDG systems may be designed to save costs and yet meet load requirements, literature evaluations show that these systems need metaheuristic methodologies with high computing power and accuracy to be successful. By using WTs and BS systems, a continuous power source may be created for a specific load. A shift in the distribution network voltages and imbalance occurred due to WBHDG injecting power into the network. Furthermore, the node voltages will be changed by the effective alteration in the load flow's impedance. Besides, the induced voltage results from changes in the line current distribution. WBHDG systems can alleviate these issues and optimize the benefit of deploying these kinds of energy-generating systems in distribution networks [31]. As mentioned before, the impact of SWBHDG optimization on PQ indices in unbalanced radial distribution networks has not been well studied in the literature. The important PQ indices taken into account in this research are voltage sag, voltage swell, harmonics, and voltage unbalance. The literature review clears that there is still a need of an optimal allocation framework for the allocation of SWBHDG energy system in the distribution network which includes a multiobjective optimization framework with a metaheuristic method with easy implementation and high effectiveness. The selected literature is reviewed and summarized in Table 1.

1.4. Contributions. In this study, the reserve energy management-based multiobjective and simultaneous two-problem SWBHDG system allocation is carried out with hybrid energy system component optimization and SWBHDG allocation in the distribution network to reduce active power loss and energy generation costs as well as to improve PQ indices such as voltage sag, voltage swell, and THD enhancement. The storage system has a significant effect on the planned energy supply in the hybrid system and has a major contribution to the cost function. Due to the high cost of using fuel cell and hydrogen storage, in this study, batteries are used for electric energy storage. A new metaheuristic optimization approach is used to simultaneously handle these two issues. The suggested approach is solved using the escaping bird search (EBS) algorithm, which takes its cues from the movements made by quick birds to evade predators. This algorithm is used to determine the decision factors, such as the SWBHDG's ideal size and location in a distribution network. The population-based EBS method searches the design space using the search agents' explicit maneuvers for the artificial predator and the prey bird. The EBS employs no operators, in contrast to the presented metaheuristic methods. Implementation of the suggested methodology is done on a distribution network with unbalanced 33-bus network. The effectiveness of the suggested methodology in achieving each aim is assessed in this study, along with the influence of some key variables on problem-solving and other objectives. Manta ray foraging optimization (MRFO) and PSO approaches are contrasted with the EBS to demonstrate its superiority in problem resolution. Additionally, the effectiveness of various hybrid energy system configurations based on various energy resources, such as SWBHDG, WBHDG (wind turbines and battery storage), and SBHDG (solar panels and battery storage), is assessed in order to improve various objectives. The key highlights of the research are presented below:

(i) Simultaneous two-problem-solving approach for allocation of the hybrid generation system

(ii) Hybrid generation system with solar and wind resources integrated with battery storage

(iii) Multiobjective function with losses, harmonic and voltage unbalance, voltage swell, and sag

(iv) Network power quality improvement with reserve energy management based on battery storage

(v) Superiority of the escaping bird search algorithm compared with PSO and MRFO

1.5. Paper Organization. Section 2 models both the charge and discharge phases of the battery storage as well as the SWBHDG system. Section 3 presents the problem formulation. The optimization strategy and how it works to solve the

Table 1: Summary of the related literature.

Ref.	System				Objective functions						Unbalanced system	Other objectives
	SP	WT	BS	DG	Losses	Voltage sag	Voltage swell	THD	Voltage unbalance	Cost		
[9]	×	×	×	✓	✓	×	×	×	×	✓	×	—
[10]	×	×	×	✓	✓	×	×	×	×	×	×	Load shedding Voltage deviation
[12]	×	×	×	✓	✓	×	×	×	×	✓	×	Voltage drop
[13]	✓	✓	×	✓	×	×	×	×	×	✓	×	Emissions Voltage deviation Voltage stability
[14]	×	×	×	✓	✓	×	×	×	×	×	×	Voltage regulation
[15]	✓	✓	×	✓	✓	×	×	×	×	×	×	—
[17]	✓	✓	×	✓	✓	×	×	×	×	✓	×	Flicker Emissions Voltage deviation
[22]	✓	✓	✓	✓	×	×	×	×	×	✓	×	—
[26]	✓	✓	✓	✓	✓	×	×	×	×	✓	×	—
[31]	✓	✓	×	✓	✓	×	×	✓	×	✓	×	Emissions
[33]	✓	✓	×	✓	✓	×	×	×	×	×	×	—
[34]	✓	✓	×	✓	✓	×	×	×	×	✓	×	System reliability
[35]	✓	✓	✓	✓	✓	×	×	×	×	✓	×	Voltage deviations
[37]	×	×	×	✓	✓	×	×	×	×	×	×	—
[40]	×	×	×	✓	✓	×	×	×	×	×	×	Power factor Voltage profile
[41]	×	×	×	✓	✓	×	×	×	×	×	×	—
[42]	×	×	×	✓	✓	×	×	×	×	✓	×	Emissions Voltage deviation
[43]	×	×	×	✓	✓	×	×	×	×	×	×	Voltage deviation Voltage stability
[44]	✓	✓	✓	✓	×	×	×	×	×	✓	×	System reliability
[45]	×	×	×	✓	✓	×	×	×	×	×	✓	—
[46]	×	×	×	✓	✓	×	×	×	✓	✓	✓	Voltage distortion, Voltage profile
[47]	×	×	×	✓	✓	×	×	×	×	✓	✓	—
Present	✓	✓	✓	✓	✓	✓	✓	✓	✓	✓	✓	—

× and ✓mean not specified and specified.

problem are described in Section 4. Results and discussion are offered in Section 5, while Section 6 presents the conclusion.

2. SWBHDG Modeling

In this paper, the standalone SWBHDG system containing wind turbines, solar panels, battery storage, and an inverter is presented in Figure 1. A SWBHDG system is designed to determine the size of wind turbines, solar panels, and battery banks which leads for minimizing production cost of the energy (PCE) and feed the load of the SWBHDG system [4, 25].

2.1. Strategy of SWBHDG Operation. A connection to the distribution network is possible for SWBHDG. A flowchart of the standalone SWBHDG system operation is depicted in Figure 2. The following describes the SWBHDG exploitation plan in relation to the distribution network:

(i) The entire energy produced by SPs and WTs is equal to load demand ($P_{SP}(t) + P_{WT}(t) = P_{D\_HDG}(t)/\eta_{Inv}$). In this case, the total power produced by the SPs and WTs is injected into the SWBHDG load through the inverter. $P_{SP}(t)$ is PV power at time (t), $P_{WT}(t)$ is WT power at time t, $P_{D\_HDG}(t)$ denotes HDG power at time t, and η_{Inv} refers to the inverter efficiency

(ii) The SWBHDG demand is larger than the entire quantity of energy produced by SPs and WTs ($P_{SP}(t) + P_{WT}(t) > P_{D\_HDG}(t)/\eta_{Inv}$). The extra power generated by the SPs and WTs is routed to the battery to be stored in this situation. If the quantity of injected power in this particular instance surpasses

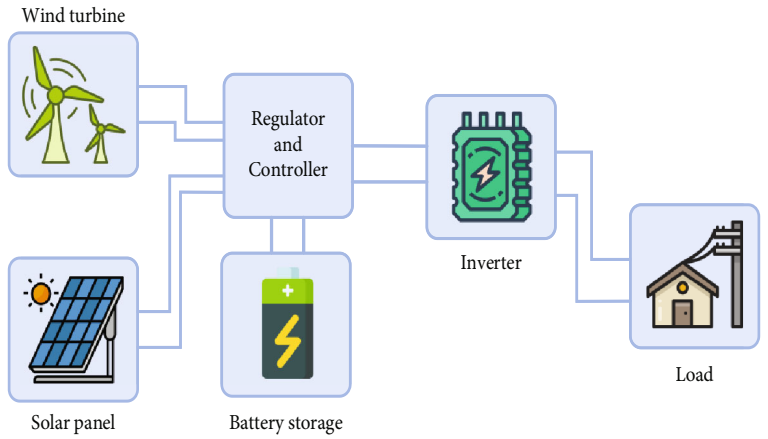

Figure 1: Block diagram of standalone SWBHDG system.

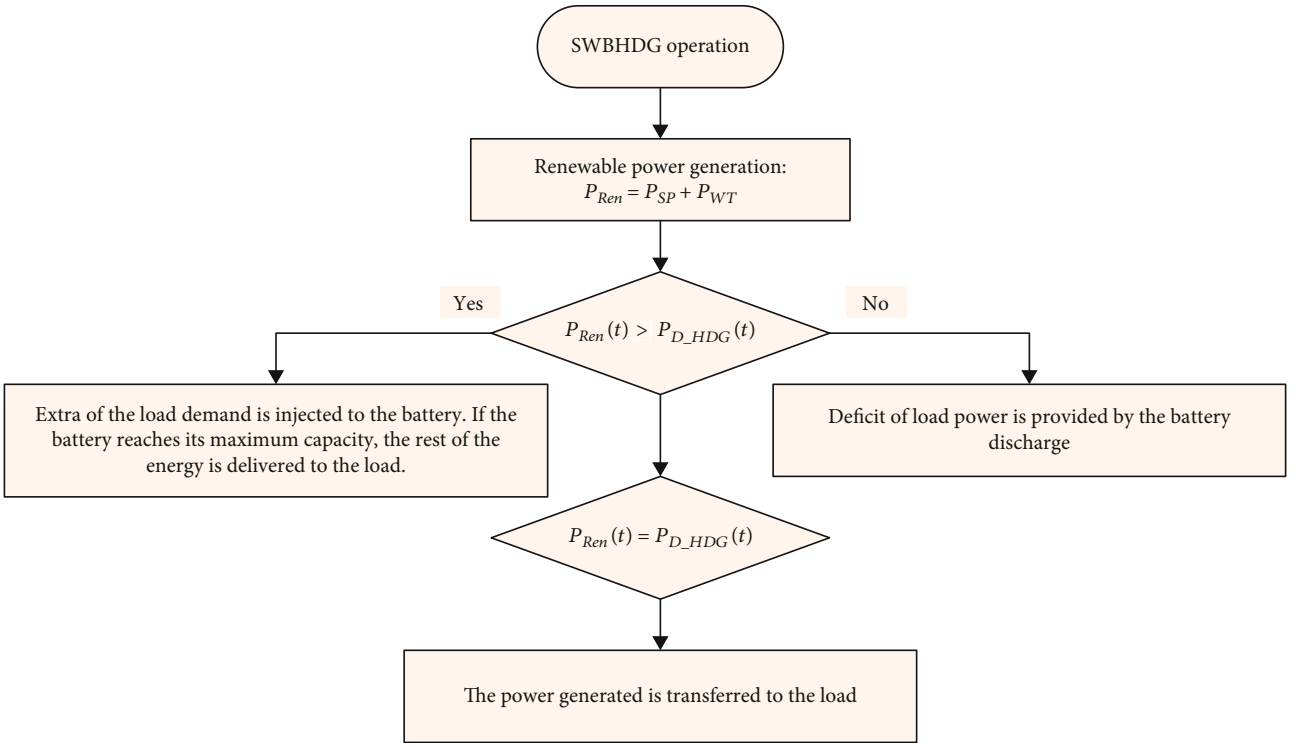

Figure 2: Flowchart of the standalone SWBHDG system operation.

the maximal battery level, the SWBHDG additional power may be injected into the distribution network

(iii) SWBHDG load demand is less than the entire quantity of energy generated by SPs and WTs ($P_{SP}(t) + P_{WT}(t) < P_{D\_HDG}(t)/\eta_{Inv}$). The BS provides the shortfall power of load demand in these circumstances. In this instance, the battery is completely discharged. If the shortfall is more than the battery's nominal capacity, a portion of the load should be reduced, resulting in a load outage. The SWBHDG load supply plan, on the other hand, is intended for complete load supply by SPs and WTs generation in this situation

The role of the battery is to compensate for power fluctuations of PV and WT sources. Because without battery storage, there is no possibility of continuous supply of load with the desired level of reliability. Therefore, it causes electrical scheduling in the hybrid system. The charging and discharging patterns of the battery storage are determined based on the power generation of renewable resources as well as the load demand during the simulation hours.

2.2. SP Modeling. According to the irradiation, the output power of each of the SPs is computed as follows [25]:

$$P_{SP} = P_{SPRated}\left(\frac{G}{1000}\right) \times [1 - k(T_C - T_{Rated})], \quad (1)$$

where G is the right irradiance to the array, P_{SPRated} shows the rated power of each SP at $G = 1000\,\text{W/m}^2$, and T_C and T_{Rated} refer to SP temperature and rated temperature, respectively. SP systems are typically equipped with MPPT systems to extract the maximum output power.

2.3. WT Modeling. The biggest advantage of wind energy is its economic efficiency. If the wind velocity surpasses the speed of v_{ci}, the WT begins to operate. The power remains fixed if the wind speed is larger than the wind turbine's nominal speed. However, the wind generator is shut down for safety reasons when the wind speed surpasses the v_{co}. A wind generator's output power is governed by v_{ci} and v_{co}, and its rated power (P_{WTRated}) is computed based on wind speed as follows [25]:

$$P_{\text{WT}} = \begin{cases} 0, & \text{if } v \le v_{\text{ci}} \text{ or } v \ge v_{\text{co}}, \\ P_{\text{WTRated}} \times \dfrac{v - v_{\text{ci}}}{v_r - v_{\text{ci}}}, & \text{if } v_{\text{ci}} \le v \le v_{r,} \\ P_{\text{WTRated,}} & \text{if } v_r \le v \le v_{\text{co}}, \end{cases} \tag{2}$$

where v refers to the wind speed and v_{ci}, v_{co}, and v_r declare the cut-in, cut-off, and nominal rapidity of the WT.

2.4. BS Modeling. In hybrid systems, batteries are applied to supply for the power shortage produced by SPs and WTs. The battery capacity is variable in hybrid systems due to the random nature of renewable resources. The state of charge (SOC) of the battery is demonstrated as follows [25]:

(i) The battery bank is in charge mode when the entire power of SPs and WTs sanded to the system is higher than the requested load of SWBHDG. At time t, the quantity of battery charge can be obtained as follows

$$\begin{aligned} \text{SOC}(t) &= \text{SOC}(t-1) + \left(\frac{P_{\text{BS}}(t)}{V_{\text{bus}}}\right) \times \Delta t, \\ P_{\text{BS}}(t) &= P_{\text{SP}}(t) + P_{\text{WT}}(t) - P_{\text{D\_HDG}}(t)/\eta_{\text{Inv}}, \end{aligned} \tag{3}$$

where V_{bus} is the DC bus voltage (V), $P_{\text{BS}}(t)$ is the battery's input/output power, and t is time step of the simulation, which is set to one hour [45]. η_{Inv} denotes the inverter's efficiency. In addition, in this research, SOC_{min} is set to 20% of the battery upper capacity and SOC_{max} is set at 100% [25].

(ii) When the total produced power of SPs and WTs is below the SWBHDG demand, the battery storage enters discharging condition. Consequently, the battery energy at the moment t can be described as follows:

$$P_{\text{BS}}(t) = \left(\frac{P_{\text{D\_HDG}}(t)}{\eta_{\text{Inv}}}\right) - P_{\text{SP}}(t) - P_{\text{WT}}(t). \tag{4}$$

3. Problem Formulation

BS is employed in the HDG system to provide SWBHDG load demand as well as for energy management. The storage system may inject additional SWBHDG electricity into the distribution network. The study's goal is to find the best decision variables of the issue, such as the ideal size and placement of the SWBHDG system, as well as the optimal capacity of SPs, WTs, and BS, to decrease grid loss and enhance PQ indices related to network operating limitations. In addition, the decrement of network losses and the expenditures of the SWBHDG system, comprising initial investment and maintenance costs, should be addressed throughout the problem-solving process. As a consequence, the issue's major aim is to improve distribution network PQ by lowering network losses and energy generation costs. The SWTHDG system is regarded as a power source by the distribution network. As a consequence, two concerns are dealt with simultaneously. The first problem is the SWBHDG system's design, which aims to reduce energy generation costs by considering full load supply. The second challenge is to improve PQ indices comprising voltage swell, voltage sag, THD, and voltage imbalance, as well as to reduce network losses by considering network operating restrictions. The EBS is then utilized to address each of these issues simultaneously. To put it another way, the optimal size and location of the SWBHDG are determined to decrease power losses and energy generation costs while simultaneously increasing PQ in the distribution network. The proposed solution is tested on a 33-bus network that is unbalanced. The challenge is treated as a multiobjective optimization problem, with the results compared before and after the SWBHDG system in the network improved. In addition, the findings of this paper are compared to the findings of former research works to verify the validity of the recommended approach.

3.1. Objective Function. The general objective function of the problem is defined as follows:

$$\begin{aligned} \text{OF} = {} & W_1\left(\frac{C_{\text{HDG}}}{C_{\text{HDG,max}}}\right) + W_2\left(\frac{P_{\text{loss}}}{P_{\text{loss,max}}}\right) \\ & + W_3\left(\frac{V_{\text{sag}}}{V_{\text{sag,max}}}\right) + W_4\left(\frac{V_{\text{swell}}}{V_{\text{swell,max}}}\right) \\ & + W_5\left(\frac{V_{\text{THD}}}{V_{\text{THD,max}}}\right) + W_6\left(\frac{V_{\text{unb}}}{V_{\text{unb,max}}}\right), \end{aligned} \tag{5}$$

where C_{HDG} and P_{loss} are the HDG system's energy-generating costs and the network's power losses, respectively. Voltage swell, voltage sag, voltage imbalance of the network, and THD of the bus are represented by the variables V_{swell}, V_{sag}, V_{unb}, and V_{THD}, respectively. Moreover, the subscript "max" denotes the maximum values of the aforementioned parameters. Besides, W_1, W_2, W_3, W_4, W_5, and W_6 are the weighting factors of losses, energy generation cost, voltage sage, voltage swell, THD of the bus voltages, and network voltage imbalance, respectively. The weight coefficient

of each of the first to sixth sections is equal to 0.2, 0.2, 0.15, 0.15, 0.15, and 0.15, respectively, based on independent executions of the optimization algorithm for different values of each of the weight coefficients.

3.1.1. Energy Generation Cost of the SWBHDG. The cost of energy generation (C_{HDG}) formulation is offered. The HDG's design target function is described as the total of the component's investment cost and maintenance and operation expenses, including SPs, WTs, and BSs, as follows:

$$\begin{aligned} C_{\mathrm{HDG}} &= C_{\mathrm{SP}} + C_{\mathrm{WT}} + C_{\mathrm{BS}}, \\ C_{\mathrm{SP}} &= C_{\mathrm{SP\_inv}} + C_{\mathrm{SP\_O\&M}}, \\ C_{\mathrm{WT}} &= C_{\mathrm{WT\_inv}} + C_{\mathrm{WT\_O\&M}}, \\ C_{\mathrm{BS}} &= C_{\mathrm{BS\_inv}} + C_{\mathrm{BS\_OM}}. \end{aligned} \tag{6}$$

The energy production costs of the HDG induced by SPs, WTs, and BSs, respectively, are represented by C_{SP}, C_{WT}, and C_{BS}. In addition, $C_{\mathrm{SP\_inv}}$, $C_{\mathrm{WT\_inv}}$, and $C_{\mathrm{BS\_inv}}$ are the initial investment expenses for SPs, WTs, and BSs, respectively. $C_{\mathrm{SP\_O\&M}}$, $C_{\mathrm{WT\_O\&M}}$, and $C_{\mathrm{BS\_O\&M}}$ represent the maintenance and operating expenses per kW/kAh of SP, WT, and BS, respectively.

3.1.2. Power Losses of the Network. Power losses of the network based on the resistance and current of the lines can be represented as follows [48]:

$$\begin{aligned} P_{\mathrm{loss}} &= RI^2, \\ I_k &= \left| \frac{V_i - V_j}{R_k + jX_k} \right|, \\ P_{\mathrm{loss}} &= \sum_{K=1}^{N_b} RI_k^2. \end{aligned} \tag{7}$$

In the above equations, R is the resistance of the lines under consideration and I is the current flowing, R_k and X_k are the kth line's resistance and reactance, respectively, and N_b is the number of lines between buses i and j.

3.1.3. Power Quality Indices

(1) Voltage Sag. To improve the voltage drop of the entire network, this study tries to escalate the average voltage drop across all buses. The voltage sag is determined by calculating the residual voltage in a bus [5]:

$$V_{\mathrm{sag}_{\mathrm{av-bus}}} = \frac{1}{m \sum_{j=1}^{m} \left(1/n \sum_{i=1}^{n} V_i^j \right)}. \tag{8}$$

Under fault conditions in bus j, the voltage of bus i is V_i^j. In addition, j is the number of possible faults and i denotes the bus number. Under voltage drop situations, $V_{\mathrm{sag}_{\mathrm{av-bus}}}$ displays the average bus voltages.

(2) Voltage Swell. The voltage swell is the opposite of Equation (8), and it is determined as a transient in RMS voltage.

(3) THD of Voltage. Total harmonic distortion is computed by applying the THD of bus voltages as follows [5]:

$$\%V_{\mathrm{THD,busi}} = \frac{V_{d,i}}{V_{\mathrm{rms},i}} \times 100, \tag{9}$$

where

$$V_{\mathrm{rms},i} = \sqrt{\left(V_{1,i}^2 + V_{d,i}^2 \right)}, \tag{10}$$

where $V_{d,i}$ refers to the distortion component of the voltage of bus i and it is calculated as follows [5]:

$$V_{d,i} = \sqrt{\sum_{h=1}^{m} V_{h,\mathrm{busi}}^2}. \tag{11}$$

(4) Voltage Unbalance. Imbalanced loads cause unbalanced network conditions. The imbalanced level of the network is computed in this article by monitoring unbalanced bus voltages as follows [5]:

$$V_{\mathrm{unb}_{\mathrm{av-bus}}} = \frac{1}{n \sum_{i=1}^{n} \left(\sum_{j=a}^{c} \left(\left| V_{neg,i} / V_{neg,i} \right| \times 100 \right) \right)}, \tag{12}$$

where

$$\begin{aligned} V_{\mathrm{pos},i} &= \frac{1}{3} \left(V_i^a + \alpha_1 V_i^b + \alpha_2 V_i^c \right), \\ V_{\mathrm{neg},i} &= \frac{1}{3} \left(V_i^a + \alpha_2 V_i^b + \alpha_1 V_i^c \right), \\ \alpha_1 &= \mathrm{complex}\,(-0.5, 0.866), \\ \alpha_2 &= \mathrm{complex}\,(-0.5, -0.866), \end{aligned} \tag{13}$$

where $V_{\mathrm{pos},i}$ is the positive sequence voltage of bus i, $V_{\mathrm{neg},i}$ is the negative sequence voltage of bus i, and V_i^jshows the jth phase voltage of the bus i.

3.2. Problem Constraints. The answer to the optimization issue is complemented by a set of technical limitations that must be obeyed throughout the optimization process's execution. The mentioned limitations may be summarized as follows.

(i) Power balance in the HDG system during the day [31]

$$\begin{aligned} \sum_{t=1}^{24} & P_{\mathrm{SP}}(t) + P_{\mathrm{WT}}(t) + P_{\mathrm{BS}}(t) + P_{\mathrm{slack}}(t) \\ & - P_{D_{\mathrm{HDG}}}(t) - P_{\mathrm{loss}}(t) - P_{D_{\mathrm{DN}}}(t) = 0. \end{aligned} \tag{14}$$

(ii) Satisfying the constraints of the SP and the WT

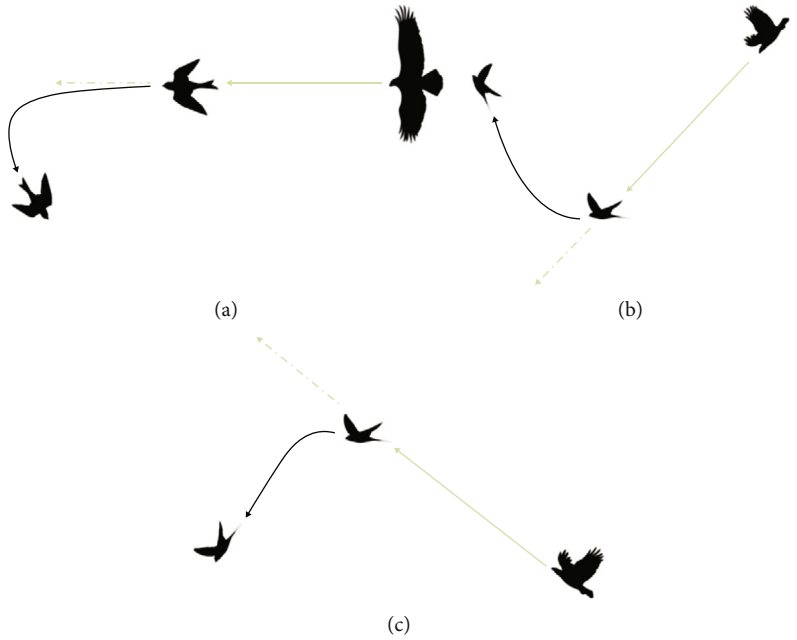

Figure 3: Escape maneuvers of the prey bird from the predator: (a) turn maneuver, (b) vertical maneuver and upward movement of the prey bird, and (c) vertical maneuver and diving movement of the prey bird [49].

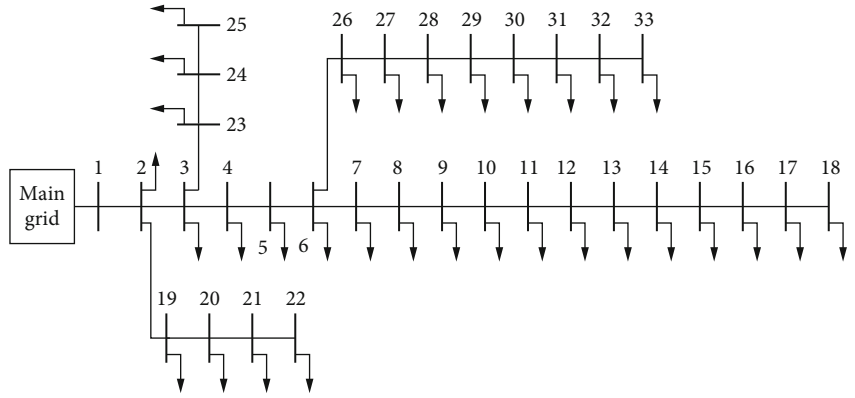

Figure 4: The 33-bus IEEE standard (unbalanced) distribution network.

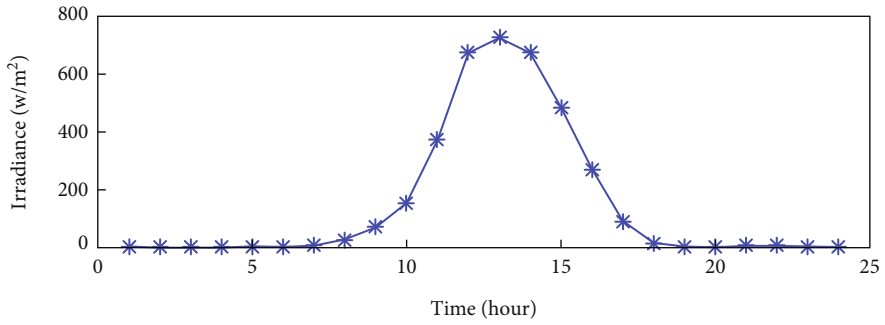

Figure 5: Irradiance profile during a day.

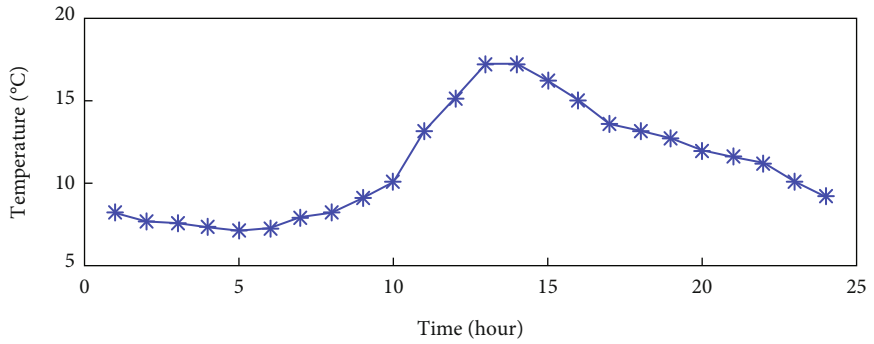

Figure 6: Temperature profile during a day.

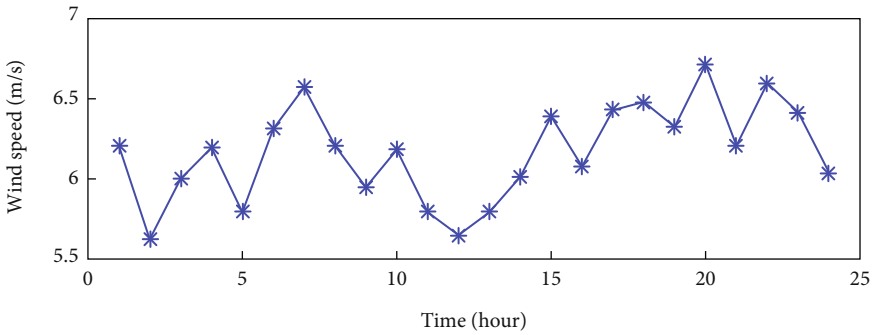

Figure 7: Wind profile during a day.

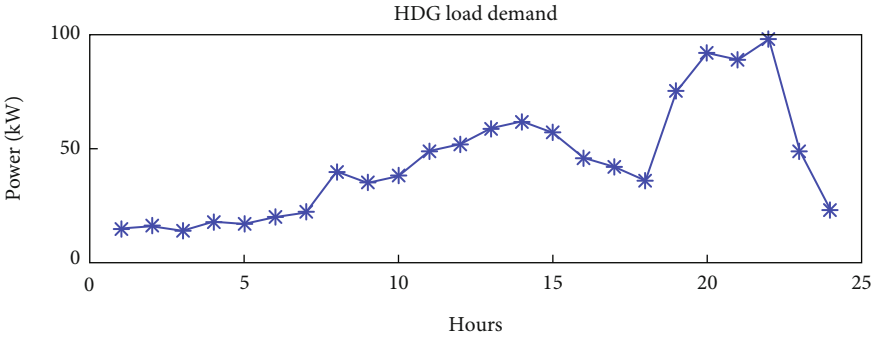

Figure 8: Load profile during a day.

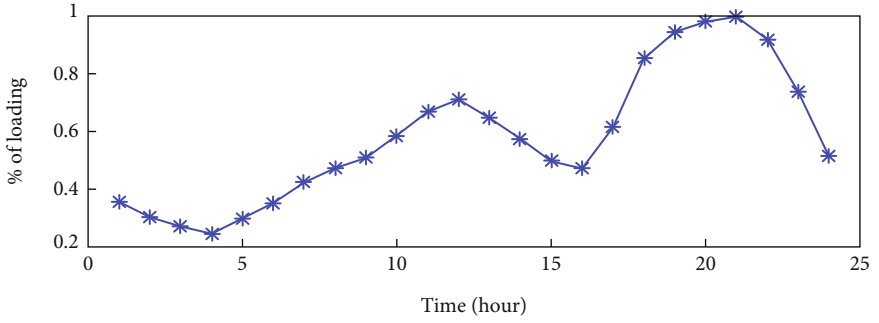

Figure 9: Normalized network load during a day.

$$0 < P_{SP} < P_{SP,max},$$
$$0 < P_{WT} < P_{WT,max}. \quad (15)$$

(iii) Satisfying the charging and discharging conditions

$$SOC_{min} < SOC(t) < SOC_{max}. \quad (16)$$

(iv) Bus voltages

$$V_{min} < V < V_{max}. \quad (17)$$

(v) Satisfying the line powers

$$F_b < Limit_b. \quad (18)$$

According to Equation (18), the current passing through each network line (F_b) should not exceed a permissible value ($Limit_b$).

$P_{SP}(t)$, $P_{WT}(t)$, $P_{BS}(t)$, and $P_{D\_HDG}(t)$ show the generated power by SP, WT, BS, and power consumption of the HDG at hour t, respectively. $P_{slack}(t)$, $P_{loss}(t)$, and $P_{D\_DN}(t)$ refer to the power supplied from the main substation of the distribution network, the power losses in the distribution network, and the power consumption of it at the time t, respectively. Furthermore, $P_{SP,max}$ and $P_{WT,max}$ are the maximum generated power by SP and WT, $SOC(t)$, SOC_{min}, and SOC_{max} are battery state of charge at time t and minimum and maximum SOC of battery, V_{min} and V_{max} refer to the minimum and maximum bus voltages, and $Limit_b$ is the thermal limit of line b and F_b which refers to power flowing from line b, respectively.

For load flow, the forward/backward sweep method was applied in this study. There are two fundamental stages in the algorithm for progressive forward load flow, which is very simple to learn and used in all radial networks. Firstly, the voltage of all the network buses is equal to 1. Then, it uses two steps to find new voltages and current flows. These two steps act as a ring and the forward sweeper in this section has been used. All the buses' voltages are considered equal to 1. The flow of each bus is easily achieved. At this step, the flow of each bus is achieved. The voltage level is updated at the conclusion of the feeder. We are aware that the voltage was set to 1 and that bus flow was obtained. Now, the same current is used to derive the new voltage at the end of the feeder. On the other hand, we know that the value of S is always constant over the whole forward/backward sweep load flow stage. Again, new voltages were obtained. It turns again to the leading forward step and then the backward step. These steps continue so that the error between the two steps, the difference in voltages, reaches a very small amount, and ultimately, the current and voltage of all branches and buses are obtained.

Table 2: SP data [25].

Parameter	Value
Type	KC200GT
$Tem_{ST\,SP}$	25°C
$Ra_{ST\,SP}$	1000 W/m^2
$P_{SPRated}$	1 kW
Temperature coefficient	-0.0037 k

Table 3: WT data [25].

Parameter	Value
Type	Bergey BWC
v_{ci}	4 m/s
v_{co}	25 m/s
$P_{WTRated}$	1 kW
v_r	13 m/s

Table 4: BS data [25].

Parameter	Value
$P_{BSRated}$	1 kAh
Vol_{BS}	12 volts
SOC_{min}	0.2 kAh
DOD	80%

Table 5: Technical and cost data of the system [25].

Parameter	PV	WT	BS
Lifetime (year)	20	20	5
Investment cost ($)	2000	3200	100
Operation and maintenance cost ($)	33	100	5

4. Proposed Optimization Method

This study presents the optimal allocation of the SWBHDG system for improving network power quality indices using the EBS [49].

4.1. Escaping Bird Search (EBS) Algorithm. Different types of living organisms have unique and advanced strategies to avoid predation. One of the birds with a smooth and continuous flight is *Apus* (swift) which uses surface and vertical maneuvers to escape from predators. In the surface maneuver, the prey bird can make fast turns to avoid being caught by a predator that attacks horizontally. In the vertical maneuver, the bird uses fast ascending flights against the diving predator. Also, the prey bird uses diving behavior against the upward movement of the predator. These two maneuvers are shown in Figure 3. In this figure, the dashed

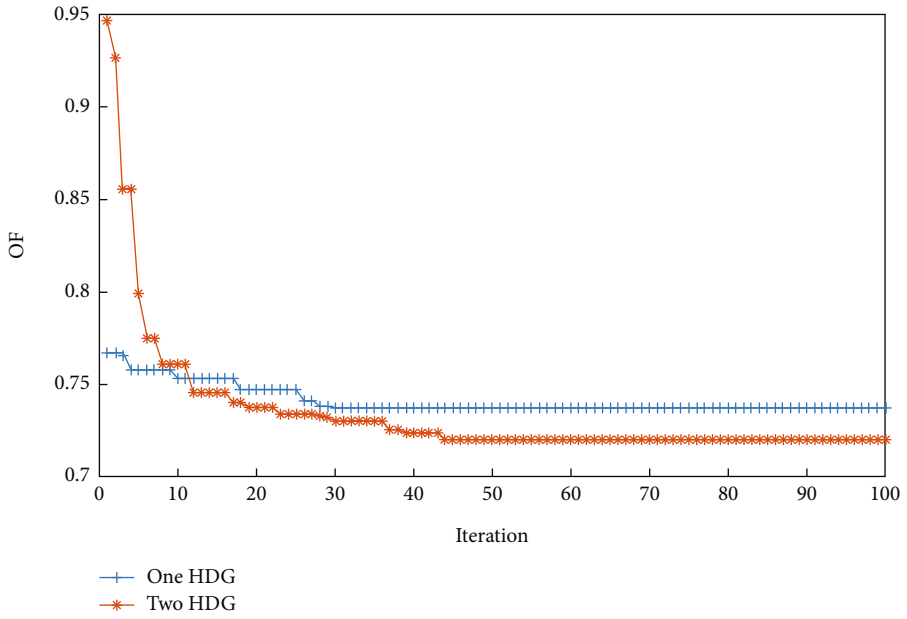

Figure 10: Convergence curve of EBS in one and two HDG multiobjective allocations in the unbalanced distribution network.

Table 6: Optimal size and site of one SWBHDG in an unbalanced 33-bus network.

Objective function	SP size (kW)	WT size (kW)	BS size (kW)	Location (bus)	Cost (M$)
min P_{loss}	253	481	610	30	10.405
min $\sum V_{sag}$	179	484	550	30	9.987
min $\sum V_{swell}$	301	490	242	15	10.713
min $\sum V_{THD}$	305	482	446	15	10.627
min $\sum V_{unb}$	361	445	689	33	10.286
min OF (multiobjective)	127	258	111	30	7.385

line represents the path of the predator after being misled by the prey bird.

The EBS algorithm is inspired by the maneuvers of the swift bird to avoid predation. The EBS algorithm is population-based, which explores the design space based on the maneuvers expressed for the prey bird and the artificial predator as search agents. A randomly selected bird from the population, with less adaptation, is considered as a prey bird and another as a predator bird. The place of the artificial bird in the search space is presented as a vector that is modified during the flight of the bird. Maneuverability of artificial bird i (MB_i) depends on factors such as the bird's body surface area (b_i), wing beat rate (β), and speed, which is modeled as follows [49].

$$MB_i = b_i \|Vel_i\|^{\beta}, \tag{19}$$

$$\|Vel_i\| = \sqrt{\sum_j Vel_{i,j}^2}, \tag{20}$$

where the velocity vector Vel_i represents the difference between the current and former places of the ith bird.

The MB depends on the wing beat rate, which is expressed by the β parameter and varies randomly between 0 and 2. The body coefficient (b_i) also presented the influence of the bird's body area (cost) in the form of the following normalized relationship [49].

$$b_i = \frac{c_{max} - c_i}{c_{max} - c_{min} + \varepsilon}, \tag{21}$$

where c_i is the cost of agent i, c_{max} and c_{min} are the maximum and minimum costs of the current population, and ε is a very small constant (provided to avoid division by zero).

According to the maneuverability of the attacking bird (AB) and the escaping bird (EB), the escape rate (ER) is modeled as follows [49]:

$$ER = \frac{MB_{EB}}{MB_{AB} + MB_{EB}}, \tag{22}$$

where MB_{AB} and MB_{EB} refer to the maneuverability of the predator bird and the prey bird, respectively.

In the process of vertical maneuvering, the prey bird selects a path in the opposite direction of the predator bird

Table 7: Results of power loss and PQ indices for one SWBHDG in an unbalanced 33-bus network.

Objective function	P_{loss} (kW)	$\sum V_{sag}$	$\sum V_{swell}$	$\sum V_{THD}$	$\sum V_{unb}$
Base net	1655.28	7.10	165.50	8.26	34.98
min P_{loss}	975.381	4.412	83.715	8.301	34.330
min $\sum V_{sag}$	2855.603	2.954	81.124	8.209	33.458
min $\sum V_{swell}$	17926	10.301	70.611	7.923	33.100
min $\sum V_{THD}$	17738	10.083	70.701	7.899	33.095
min $\sum V_{unb}$	19124	6.462	76.382	8.155	32.429
min OF (multiobjective)	1087.275	4.246	83.402	8.239	34.216

Table 8: Optimal size and site of one and two HDG placement in an unbalanced 33-bus distribution network with a multiobjective function.

Number of HDG	SP size (kW)	WT size (kW)	BS size (kW)	Location (bus)
One	127	258	111	30
Two	201, 111	164, 312	4, 15	30, 11

Table 9: Results of one and two HDG placements in an unbalanced 33-bus network with a multiobjective function.

Number of HDG	P_{loss} (kW)	System cost (M$)	$\sum V_{sag}$	$\sum V_{swell}$	$\sum V_{THD}$	$\sum V_{unb}$
One	1087.275	7.385	4.246	83.402	8.239	34.216
Two	1072.617	10.642	4.016	83.205	8.224	34.179

to mislead it. The presented artificial flight is modeled as follows:

$$PO_{EB} = PO_{EB} + r \times ER \times (Opp(PO_{AB}) - PO_{EB}), \quad (23)$$

where PO_{AB} and PO_{EB} represent the positions of predator and prey birds, r refers to a random value created with a uniform distribution between 0 and 1, and ER represents the escape rate.

The Opp(PO) function expresses the opposite value of a vector in the search space, which is defined as follows [49]:

$$Opp(PO_{AB}) = PO_L + PO_H - PO_{AB}. \quad (24)$$

In the condition of small ER, the prey bird executes the surface maneuver by changing the direction of its current position. This maneuver is modeled as follows:

$$PO_{EB} = PO_L + r \times (PO_H - PO_L), \quad (25)$$

where PO_L and PO_H represent the low and high values of the vector of variables, respectively, and r is a vector with random values in the range between 0 and 1.

In the process of evolution of the simulation, the flight towards the best global experience of all prey so far (PO_{Gbest}) has been added; thus, the bird of prey maneuver is presented as follows [49]:

$$PO_{AB}^{Candidate} = PO_{AB} + r_1 \times (PO_{EB} - PO_{AB}) + r_2 \times (PO_{Gbest} - PO_{EB}), \quad (26)$$

where r_1 and r_2 are randomly generated in the range of 0 and 1. The capturing rate (CR) is presented as follows:

$$CR = 1 - ER. \quad (27)$$

In the condition of a high ER value, the value of CR is zero and vice versa.

Equation (27) represents an update of the summation position, which is a stepping behavior in some methods such as the PSO algorithm. But, in the EBS algorithm, instead of the adaptive and inertia coefficients of PSO, only a CR adaptation coefficient is used.

The steps of the EBS algorithm based on the simulated maneuvers of artificial birds of prey and predator are presented as follows:

(1) Step (1) Random population generation of N artificial birds. The ith bird is produced as follows according to the upper and lower range of the design variables

$$PO_i = PO_L + r \times (PO_H - PO_L). \quad (28)$$

(2) Step (2) The amount of each MB is calculated based on Equation (19) and the normalized cost values in Equation (21)

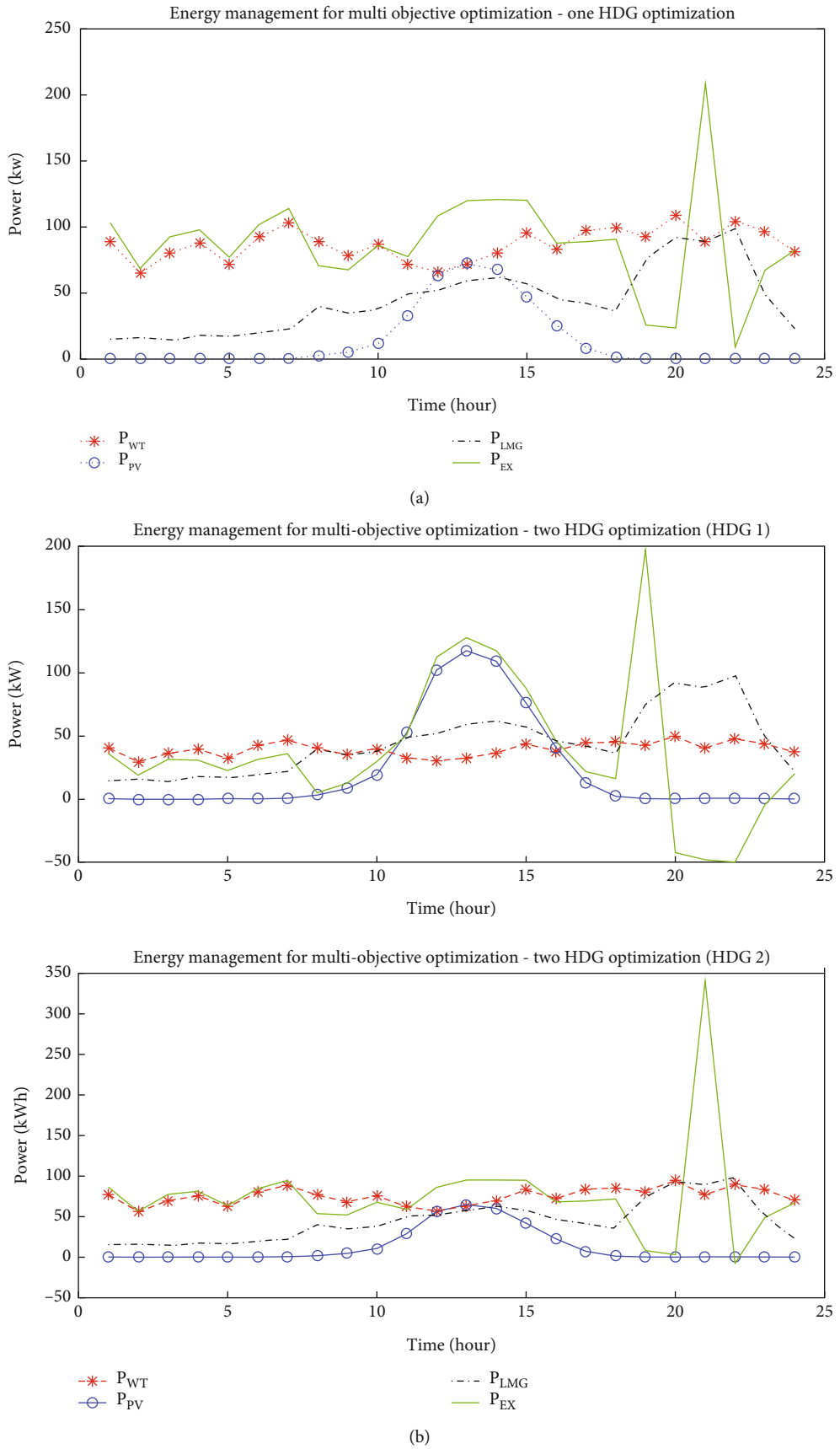

Figure 11: Energy management due to SWTBAHDG allocation in 33-bus network: (a) one SWBHDG and (b) two SWBHDGs.

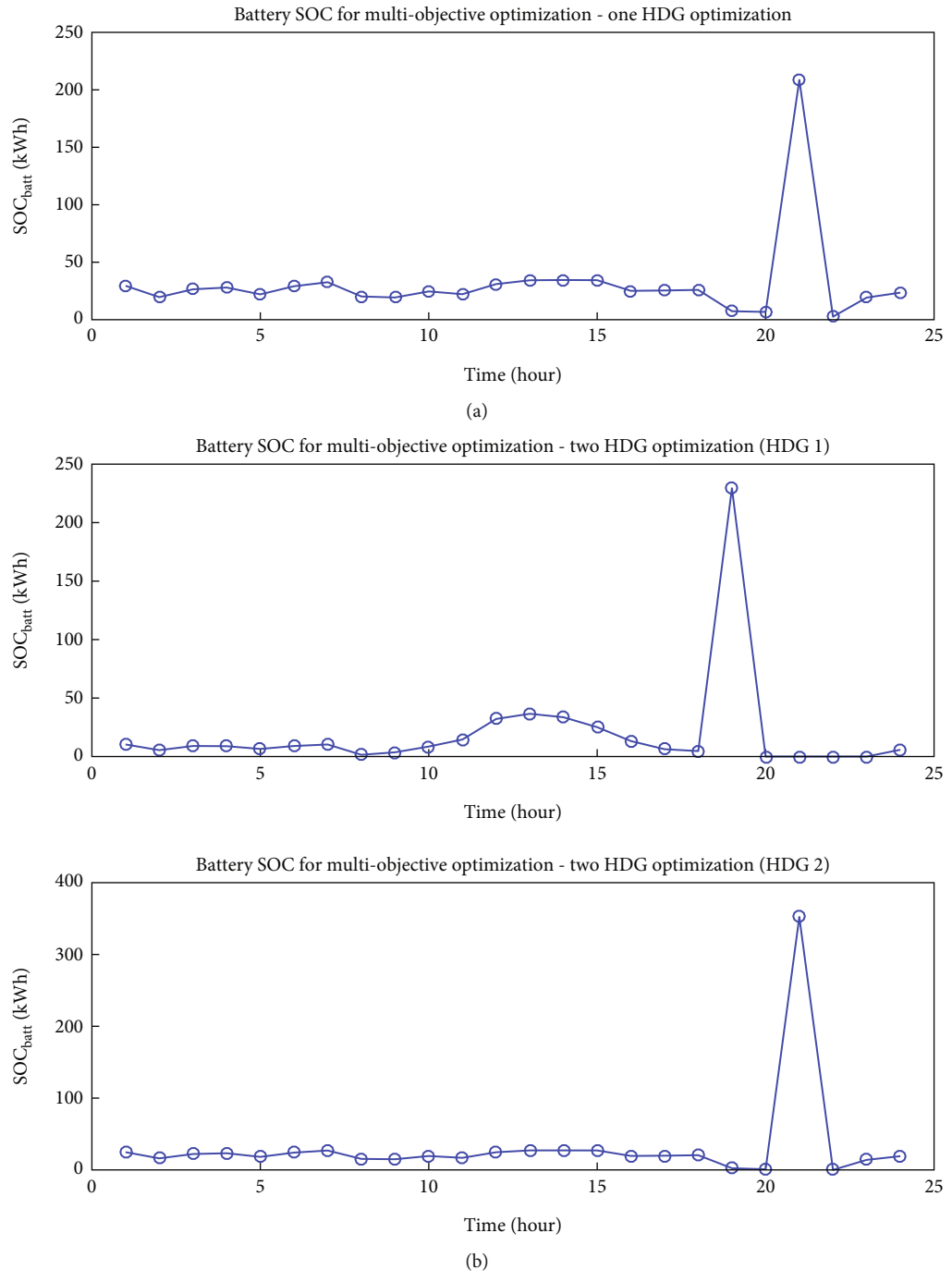

Figure 12: Variation of battery for SWBHDG allocation in 33-bus network: (a) one SWBHDG and (b) two SWBHDGs.

(3) Step (3) The above main loop is executed until the convergence conditions are satisfied as follows:

(i) For i as many as N artificial birds, the operation should be performed

(ii) The best bird should be selected as AB and the worst as EB

(iii) Calculate MB, ER, and CR parameters for AB and EB birds

(iv) Provide a candidate solution for AB based on Equation (26)

(v) Calculate the cost of $PO_{AB}^{Candidate}$

(vi) In a condition that the amount of $PO_{AB}^{Candidate}$ cost is less compared to PO_{AB}, PO_{AB} replaces it

(vii) Exit the loop after completing the number of cost function evaluations (NCFE) relative to the default value

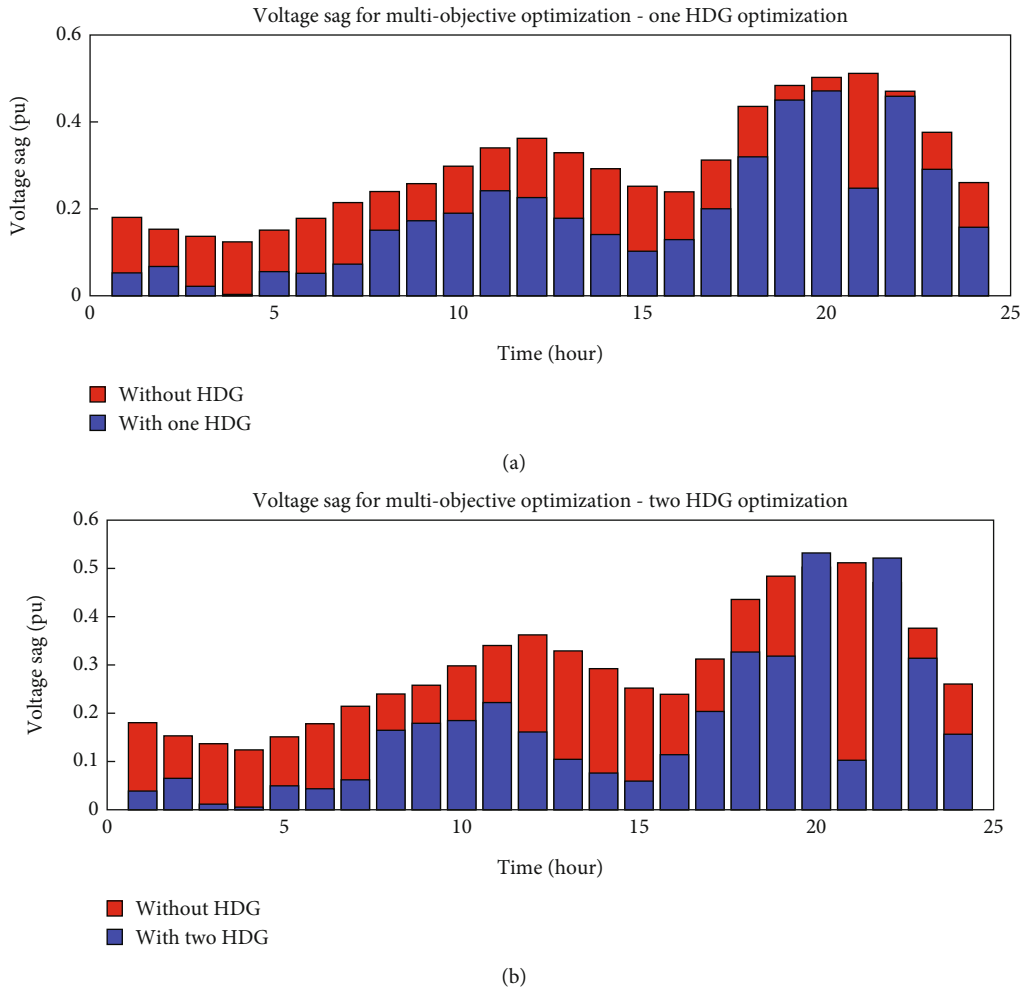

Figure 13: Effect of SWBHDG allocation in a 33-bus network on voltage sag: (a) one SWBHDG and (b) two SWBHDGs.

(viii) For EB based on either surface maneuver or vertical maneuver, a candidate solution is generated. The transition between the described maneuvers is modeled as follows [49]:

$$PO_{EB}^{Candidate} = \begin{cases} PO_L + r \times (PO_H - PO_L), & \text{if } ER < \frac{1}{N}, \\ PO_{EB} + r \times ER \times (Opp(PO_{AB}) - PO_{EB}), & \text{otherwise.} \end{cases} \quad (29)$$

(ix) Calculate the cost of $PO_{AB}^{Candidate}$

(x) In the case of lower cost of $PO_{AB}^{Candidate}$ compared to PO_{EB}, PO_{EB} replaces it

(xi) Exit from the main loop as soon as NCFE reaches $NCFE_{max}$

(xii) PO_{Gbest} update

(xiii) In the condition $i = N$ and $NCFE < NCFE_{max}$, go to Step 3. If not, exit the loop and go to Step 4

(4) Step (4) In this step, the updated PO_{Gbest} is saved as the optimal solution

4.2. The EBS Implementation. The proposed EBS optimization algorithm seeks to determine the optimal set of optimization variables by minimizing the objective function (Equation (5)) and satisfying the constraints Equations (14)–(18) of the problem. Therefore, the proposed algorithm is looking for the optimal solution in the allowed range of decision variables, with the aim of reaching the minimum value of the objective function and in this condition also meeting the constraints of the problem.

The steps of the EBS for problem solving are as follows:

(i) Step (1) Define the decision variables and constraints, including the maximum number of iterations and EBS parameters

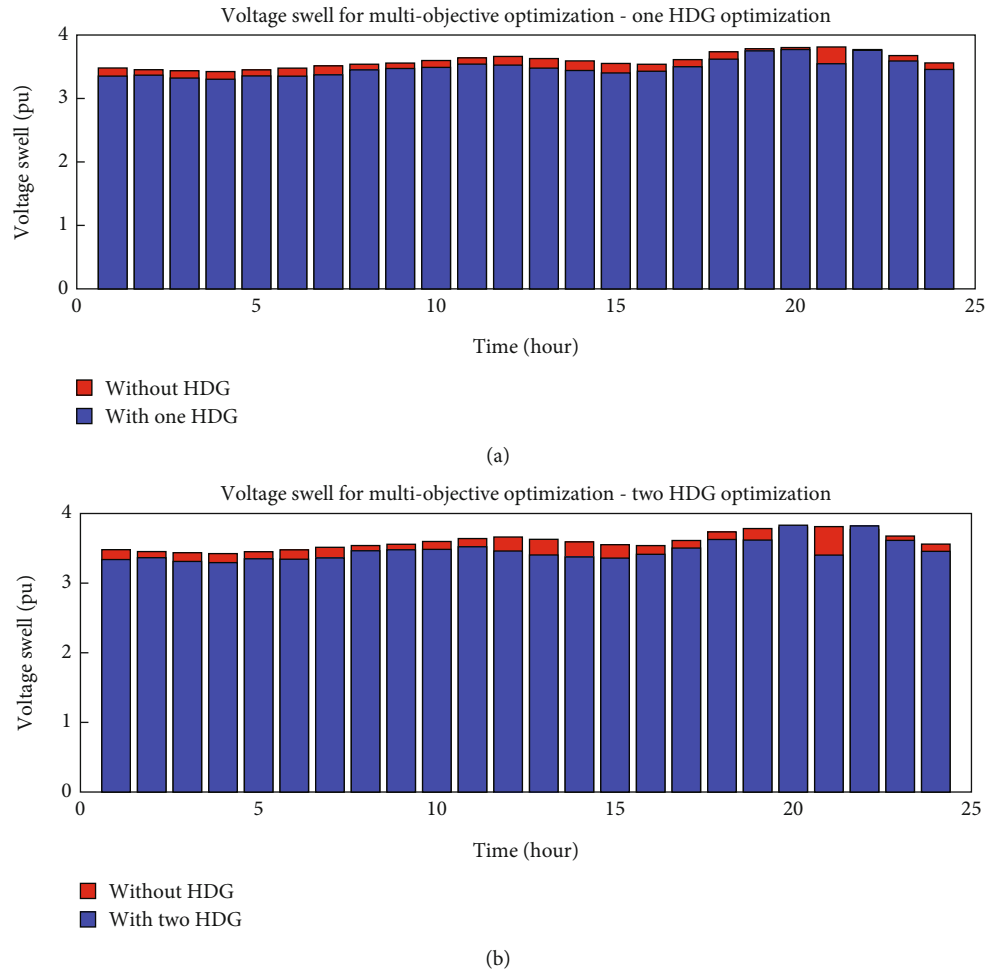

Figure 14: Effect of SWBHDG allocation in a 33-bus network on voltage swell: (a) one SWBHDG and (b) two SWBHDGs.

(ii) Step (2) Examining the principal circumstance of the randomly selected population

(iii) Step (3) The objective function is evaluated and the objective values for each population member are calculated

(iv) Step (4) Equation (23) is used to declare the new status of each member of the population

(v) Step (5) The population member's position will be updated if the acquired locations fall within the search range

(vi) Step (6) The new value of the objective function is determined based on the new circumstances of each population member

(vii) Step (7) The EBS is updated. If the population members achieve a higher position than previously recorded, replace them with the new information

(viii) Step (8) If convergence criteria are met, proceed to Step 9, otherwise repeat Steps 4 through 8.

(ix) Step (9) Stop the EBS and print the best results

5. Simulation Results and Discussion

This section presents the simulation results of SWBHDG allocation based on SPs and WTs with BS to enhance power quality indices in an unbalanced 33-bus radial distribution network. Figure 4 depicts the single-line diagram of the IEEE standard 33-bus network.

The overall power usage in the 33-bus network is 3720 kW and 2300 kVAr. There are 37 branches in the 33-bus network. Moreover, it is comprised of the main branch and three subbranches [45]. Figures 5–7 show the data variations. Figures 8 and 9 show the SWBHDG load curve with a 100 kW peak as well as the network's normalized load.

Tables 2–4 show the technical data for the SPs, WTs, and BSs, respectively. Table 5 also includes technical and economic statistics for the HDG system's components [25].

5.1. Results of One and Two HDG Optimizations. The single and multiobjective allocation results of one SWBHDG via the EBS are reported in this section. Figure 10 depicts the convergence curve of EBS in one and two SWBHDG multiobjective optimizations in an imbalanced 33-bus distribution network. The optimization process employing the

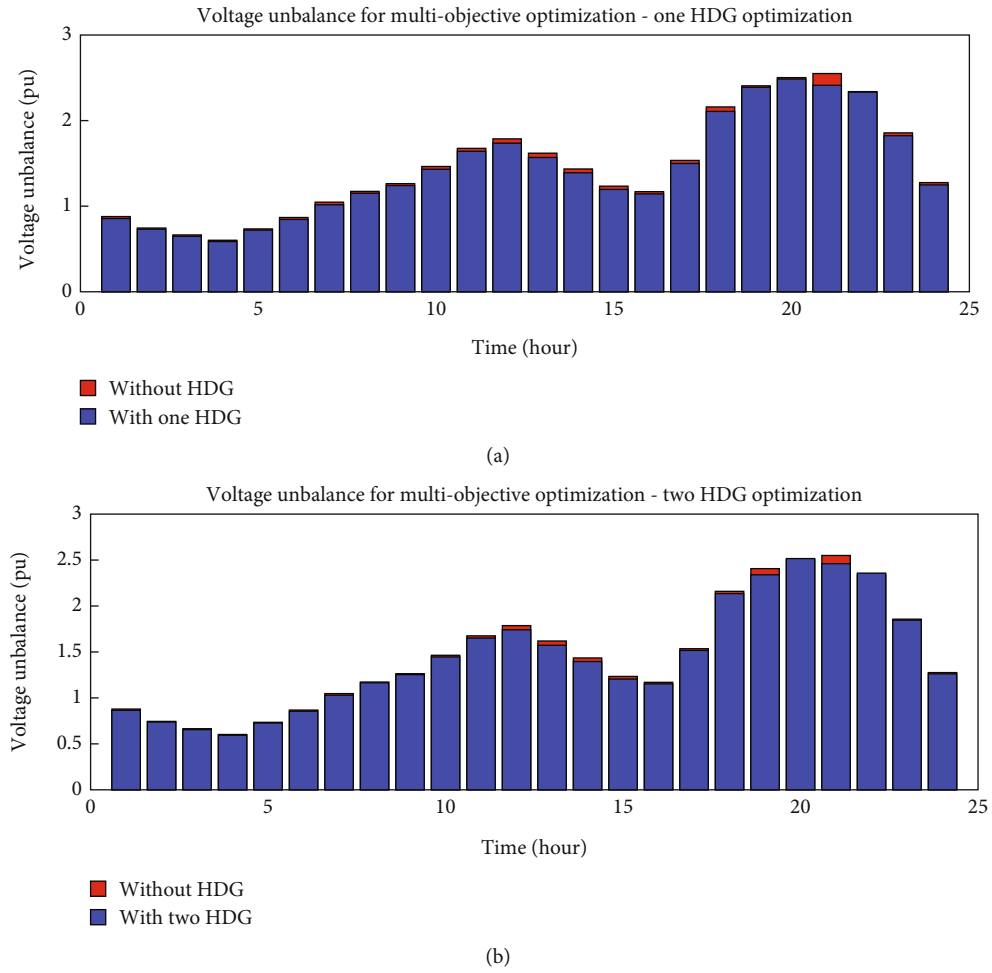

Figure 15: Effect of SWBHDG allocation in a 33-bus network on voltage unbalance: (a) one SWBHDG and (b) two SWBHDGs.

suggested method in various iterations and optimum solution accomplishment is shown in Figure 10. As can be shown, a rise in HDGs has resulted in a drop in objective function or improved physical attainment.

Tables 6 and 7 display the results of a single-objective and multiobjective optimization of one SWBHDG using the EBS, including the size and position of one SWBHDG, as well as power loss, SWBHDG system cost, voltage surge, voltage drop, voltage imbalance, and total harmonic distortion (THD). The results indicate that WTs have a greater impact in SWBHDG and that bus 30 is the optimal site for installing SWBHDG. In addition, 7.385 M$ is the shortest cost for SWBHDG when multiobjective optimization is applied to the problem-solving procedure.

The simulation results revealed that a loss reduction target function with a singular aim yields the lowest loss. Consideration of a single optimization has a positive impact on all PQ indicators. Using the single optimization for PQ indices appears to have a negative impact on power loss reduction. All PQ indices are enhanced by addressing voltage sag and voltage imbalance as a single-objective optimization function. On the other hand, voltage sag is reduced in voltage surge and THD target optimization. The voltage sag objective function returns the value with the lowest voltage sag. The function value of voltage sag has a considrable impact on other PQ indicators relative to the base value, but it also increases network losses. By contemplating the voltage increase as a single-objective optimization, the minimum value of voltage is attained in this instance. On the other hand, only the objective function of voltage expansion has a considerable impact on voltage imbalance and THD, reducing them relative to the base value. It has a negative effect on cost, voltage drop, and loss, however. In the THD optimization, the minimum THD is attained. The THD function has a substantial effect on voltage imbalance and voltage swell, but no effect on the other indices. The objective function of voltage imbalance improves all PQ indices, excluding power loss. In addition, the ideal voltage imbalance is achieved in this scenario. All target functions are merged and normalized during multiobjective optimization. When one SWBHDG is multiobjectively optimized in a 33-bus distribution network, the power loss is declined, all PQ indices improve, and the lowest SWBHDG cost is attained. Consequently, incorporating the multiobjective problem improves PQ. As a result, multiobjective optimization is a more practical and accurate approach to solving a problem in which all of its objectives are satisfied.

In addition, the optimization of two SWBHDG in a 33-bus distribution network is performed, and the obtained

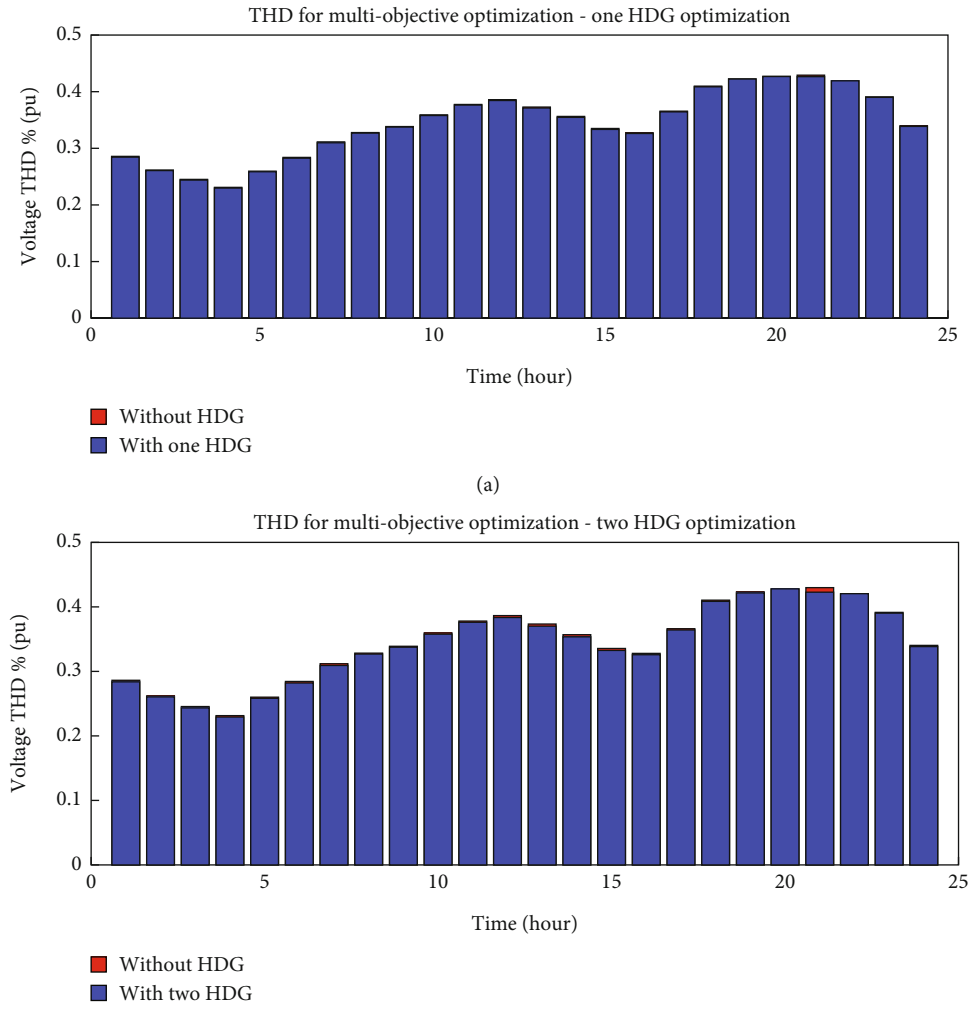

Figure 16: Effect of SWBHDG allocation in the 33-bus network on THD: (a) one SWBHDG and (b) two SWBHDGs.

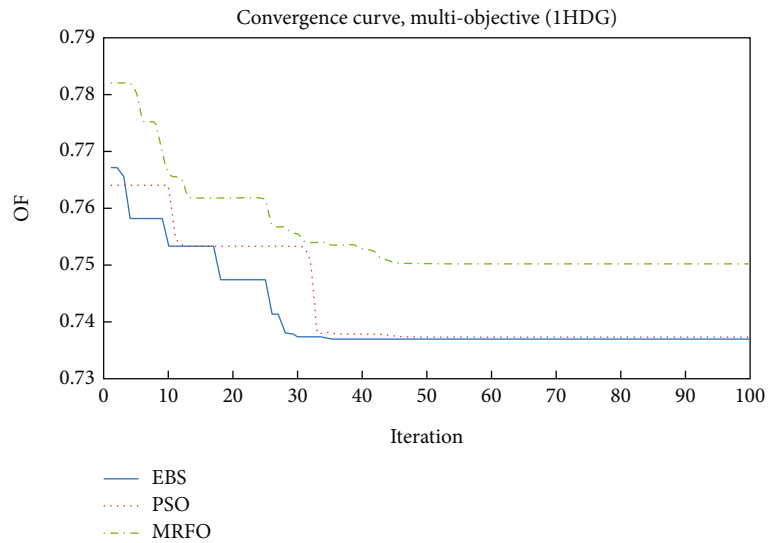

Figure 17: Convergence process of a different method with multiobjective optimization (one SWBHDG).

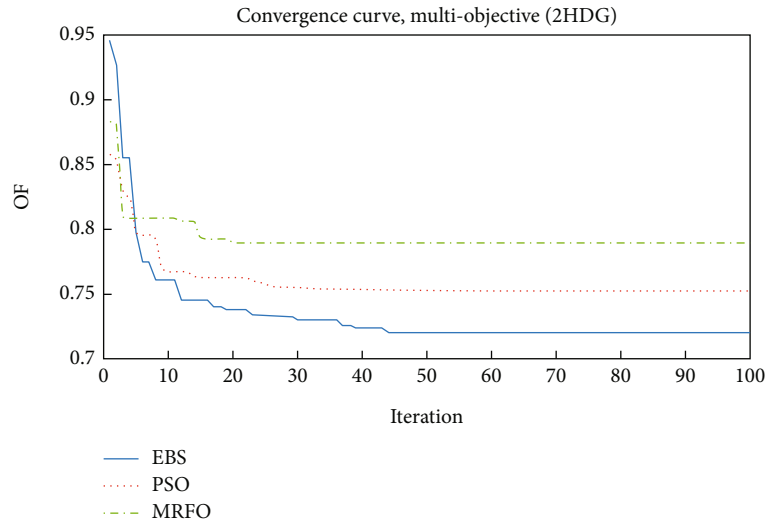

Figure 18: Convergence process of a different method with multiobjective optimization (two SWBHDGs).

Table 10: Comparison of optimal size and site of one SWBHDG in a 33-bus network with multiobjective via different optimization methods.

Optimization method	SP size (kW)	WT size (kW)	BS size (kW)	Location (bus)	Cost (M$)
EBS	127	258	111	30	7.385
PSO	114	389	380	30	7.871
MRFO	87	356	83	30	7.134

Table 11: Comparison of results of one SWBHDG allocation in a 33-bus network with multiobjective using different optimization methods.

Optimization method	P_{loss} (kW)	$\sum V_{sag}$	$\sum V_{swell}$	$\sum V_{THD}$	$\sum V_{unb}$
EBS	1087.275	4.246	83.402	8.239	34.216
PSO	1133.520	4.583	83.48	8.235	34.301
MRFO	1108.950	4.65	83.85	8.236	34.26

Table 12: Comparison of optimal size and site of two SWBHDG in a 33-bus network with multiobjective using different optimization methods.

Optimization method	SP size (kW)	WT size (kW)	BS size (kW)	Location (bus)	Cost (M$)
EBS	201, 111	164, 312	4, 15	30, 11	10.642
PSO	205, 135	308, 147	58, 7	32, 28	10.378
MRFO	269, 79	233, 26	64, 0	31, 2	6.765

results are contrasted with the optimization of a single SWBHDG, according to Tables 8 and 9. The sizes of two SWBHDG are presented, and the results of one SWBHDG optimization are compared. As it is clear, the cost of with two SWBHDG is greater than the optimal implementation of a single SWBHDG, but the values of power loss and PQ indices are superior to those of a single SWBHDG. Clearly, all indices are enhanced by implementing two SWBHDG optimizations.

Energy management and contribution of the HDG components and power transferred to the network are shown in Figure 11 for one and two SWBHDG. Also, the SOC of the battery storage is illustrated for one and two SWBHDG optimizations in Figure 12. Moreover, voltage sag, voltage swell, voltage unbalance, and THD without and with SWBHDG are depicted in Figures 13–16. These figures show an improvement in PQ indices with the optimal application of one and two SWBHDG. Also, these figures show more improvement in PQ indices and also power loss reduction with two SWBHDG in comparison with one SWBHDG optimization.

5.2. Evaluation of EBS Performance. The performance of EBS in one and two SWBHDG multiobjective allocation is

Table 13: Comparison of results of two SWBHDG placements in a 33-bus network with multiobjective using different optimization methods.

Optimization method	P_{loss} (kW)	$\sum V_{sag}$	$\sum V_{swell}$	$\sum V_{THD}$	$\sum V_{unb}$
EBS	1072.617	4.016	83.205	8.224	34.179
PSO	1205.868	5.371	83.541	8.258	34.607
MRFO	1077.78	5.438	84.638	8.261	34.649

Table 14: Impact of network load increasement on one SWBHDG optimal sizing and cost results as multiobjective.

Loading level	SP size (kW)	WT size (kW)	BS size (kW)	Location (bus)	Cost (M$)
Rated network load	127	258	111	30	7.385
20% increasement	121	441	722	30	8.882

Table 15: Impact of network load increasement on one SWBHDG optimization results as multiobjective.

Loading level	P_{loss} (kW)	Cost (M$)	$\sum V_{sag}$	$\sum V_{swell}$	$\sum V_{THD}$	$\sum V_{unb}$
Rated network load	1087.275	7.385	4.246	83.402	8.239	34.216
20% increasement	1538.310	8.882	5.153	84.321	8.827	34.242

Table 16: Results of size and cost of one HDG optimization by considering different combinations as multiobjective.

Combination	SP size (kW)	WT size (kW)	BS size (kW)	Location (bus)	Cost (M$)
SWBHDG	127	258	111	30	7.385
WBHDG	—	408	1390	30	7.594
SBHDG	612	—	1584	30	7.877

Table 17: Results of one HDG optimization considering different combinations as multiobjective.

Combination	P_{loss} (kW)	$\sum V_{sag}$	$\sum V_{swell}$	$\sum V_{THD}$	$\sum V_{unb}$
SWBHDG	1087.275	4.246	83.402	8.239	34.216
WBHDG	1205.595	4.782	83.936	8.223	34.346
SBHDG	1269.570	4.794	84.105	8.224	34.472

compared to PSO and MRFO techniques in this section. The numerical results of the design and placement of one and two SWBHDG and PQ indices values are shown, as well as the convergence curves of the optimization techniques. In contrast to other approaches, the EBS method achieves a greater objective function value, as shown in Figures 17 and 18.

In contrast to the PSO and MRFO, the EBS delivers reduced losses and improved PQ indices, according to the simulation findings presented in Tables 10–13. Furthermore, for one SWBHDG design and location, all optimization algorithms choose bus 30 to install SWBHDG. Moreover, using the EBS approach, buses 30 and 11 are selected for the design and placement of two SWBHDGs.

5.3. Impact of Network Load Increasement. The impact of increased demand on multiobjective allocation of one SWBHDG is investigated in this section. According to Tables 14 and 15, when the network load grows, so does the amount of SWBHDG and the value of losses. The PQ indexes have weakened as well.

5.4. Impact of HDG Combinations. The results and positioning of multiple HDG combinations in the 33-bus unbalanced distribution network are analysed in this section. Tables 16 and 17 show the size and optimization outcomes. The findings suggest that combining SWB with both HDG-based renewable units reduces costs and losses while improving PQ indicators.

5.5. Comparison with Other Methods. The proposed EBS is compared to various solutions for minimizing unbalanced 33-bus network losses in this section. The proposed technique in this research resulted in a power loss of 1087.275 kW during 24 hours. Over an hour, the average power loss is 45.303 kW. The EBS results are compared with AACO, FGA, and MHA techniques in Table 18. The EBS recommended strategy, which is based on SWBHDG design

Table 18: Comparison with previous studies for an unbalanced 33-bus network.

Optimization method	P_{loss} (kW)	$\sum V_{swell}$	$\sum V_{THD}$
EBS	**45.303**	**83.402**	**8.239**
AACO [45]	143.870	—	—
FGA [46]	148.69	—	13.307
MHA [47]	142.71	—	—

and network placement, has lower losses and an improvement in the PQ index than the other ways, according to the data.

6. Conclusions

In this study, the design and allocation of the HDGs are performed to minimize the energy losses and enhance PQ indices in an unbalanced 33-bus distribution network. The objective of the HDG allocation is to reduce energy losses and improve the voltage sag and swell and harmonic and voltage unbalance of the network by determining the optimal size and location of the HDG components during 24 hours considering multiobjective optimization and using the EBS algorithm. The proposed methodology is implemented as single- and multiobjective allocation to show the effectiveness of the EBS via multiobjective optimization.

(i) According to the findings, the establishment of multiobjective optimization allocation using the HDGs and the integration of energy resource generation with battery reserve energy via the EBS has achieved a favorable compromise between different objectives compared to single-objective allocation; whereas in single-objective allocation, some objectives have exceeded the basic value. In addition, combining energy sources as well as number of HDG increasing has led to more enhancement of PQ indices and further decreasing the energy losses

(ii) Besides, the better capability of the proposed methodology based on the EBS in the optimal system allocation compared to other methods has been confirmed by further improving the network performance and achieving better objectives

(iii) The superior capability of the EBS is verified in comparison with the PSO and MRFO in improving the network power quality. In addition, the simultaneous combination of solar panel-wind sources integrated with the battery compared to hybrid system combinations has led to achieving better PQ indices

(iv) Therefore, the overlapping of energy resources with the storage elements has helped to enhance the network power quality

(v) The hybrid system allocation to improve power quality indices with the uncertainty of resource generation and the network load is suggested for future work

Abbreviations

HDG: Hybrid distributed generation
SP: Solar panel
WT: Wind turbine
BS: Battery storage
SWBHDG: A HDG system consists of SP, WT, and BS
PQ: Power quality
EBS: Escaping bird search
PSO: Particle swarm optimization
MRFO: Manta ray foraging optimizer
RES: Renewable energy resource
GA: Genetic algorithm
ISA-PSO: Improved simulated annealing PSO
ABC: Artificial bee colony
NRLF: Newton-Raphson load flow
AHA: Artificial hummingbird algorithm
ALO: Ant lion optimizer
CSA: Crow search algorithm
MO&O: Modified perturb and observe
MFPA: Modified flower pollination algorithms
THD: Total harmonic distortion
AEFA: Artificial electric field algorithm
IHSA: Improved harmony search algorithm
BBA: Big bang algorithm
IMFO: Improved moth flame optimization
GWO: Grey wolf optimizer
MPPT: Maximum power point tracking
ICA: Imperialist competitive algorithm
GOA: Grasshopper optimization algorithm
SSA: Spring search algorithm
EGC: Energy generation cost
SOC: State of charge
AACO: Adaptive ant colony optimization
FGA: Combined GA methodology and fuzzy logic
MHA: Modified heuristic algorithm.

Variables, Parameters, and Symbols

P_{SP}: Output power of SP
$P_{SPRated}$: Rated power of each SP
G: Right irradiance to the SP arrays
T_C: SP temperature
T_{Rated}: Rated temperature
P_{WT}: Output power of WT
$P_{WTRated}$: Rated power of WT
v: Wind speed
v_r: Rated rapidity of the WT
v_{ci}: Cut-in rapidity of the WT
v_{co}: Cut-off rapidity of the WT
P_{BS}: Input/output power of BS
V_{bus}: DC bus voltage (V)
t: Simulation time step
η_{Inv}: Inverter's efficiency
P_{D_HDG}: Output power of HDG
SOC: State of charge
OF: Objective function
W_i: Weighting factors
C_{HDG}: Energy generating costs of HDG system

P_{loss}: Power loss of the network
V_{sag}: Voltage sag
V_{swell}: Voltage swell
V_{THD}: THD of the bus voltage
V_{unb}: Voltage imbalance of the network
C_i: Cost of energy generation system i
C_{i_inv}: Initial investment expenses for energy generation system i
$C_{i\_O\&M}$: Maintenance and operating expenses for energy generation system i
R: Resistance of the line
X: Reactance of the line
I: Current of the line
N_b: Number of branches
V_i^j: Voltage of bus i under fault conditions in bus j
P_{slack}: Power supplied from the main grid
P_{D_DN}: Power consumption of the distribution network
F_b: Power flowing from line b
$Limit_b$: Thermal limit of line b
MB_i: Maneuverability of artificial bird i
Vel_i: Velocity vector of bird i
b_i: Body surface area of bird i
β: Wing beat rate
c_i: Cost of agent i
ER: Escape rate
PO_i: Position of bird i
r: A random value between 0 and 1
$Opp(.)$: Function expresses the opposite value of a vector (as its input)
CR: Capturing rate.

Data Availability

The data used in this paper for providing the study outcomes are given within the paper (Tables 2–5).

Conflicts of Interest

The authors declare that they have no conflicts of interest.

Authors' Contributions

Mohammad Jafar Hadidian Moghaddam was responsible for the conceptualization, methodology, software, and writing the original draft. Mohammad Bayat was responsible for the methodology, software, supervision, and writing the review and editing. Amin Mirzaei was responsible for the software, investigation, and validation. Saber Arabi Nowdeh was responsible for the software and writing the original draft. Akhtar Kalam was responsible for the investigation, validation, supervision, and writing the review and editing.

References

[1] D. K. Patel, D. Singh, and B. Singh, "Impact assessment of distributed generations with electric vehicles planning: a review," *Journal of Energy Storage*, vol. 43, article 103092, 32 pages, 2021.

[2] S. A. Nowdeh, A. Naderipour, I. F. Davoudkhani, and J. M. Guerrero, "Stochastic optimization–based economic design for a hybrid sustainable system of wind turbine, combined heat, and power generation, and electric and thermal storages considering uncertainty: a case study of Espoo, Finland," *Renewable and Sustainable Energy Reviews*, vol. 183, article 113440, 2023.

[3] S. O. Sanni, M. F. Akorede, and G. A. Olarinoye, "Strength assessment of electric power systems containing inverter-based distributed generation," *Electric Power Systems Research*, vol. 207, article 107825, 2022.

[4] A. Bukar and C. W. Tan, "A review on stand-alone photovoltaic-wind energy system with fuel cell: system optimization and energy management strategy," *Journal of Cleaner Production*, vol. 221, pp. 73–88, 2019.

[5] Y. Ch, S. K. Goswami, and D. Chatterjee, "Effect of network reconfiguration on power quality of distribution system," *International Journal of Electrical Power & Energy Systems*, vol. 83, pp. 87–95, 2016.

[6] M. J. H. Moghaddam, A. Kalam, S. A. Nowdeh, A. Ahmadi, M. Babanezhad, and S. Saha, "Optimal sizing and energy management of stand-alone hybrid photovoltaic/wind system based on hydrogen storage considering LOEE and LOLE reliability indices using flower pollination algorithm," *Renewable Energy*, vol. 135, pp. 1412–1434, 2019.

[7] M. Khajehzadeh, M. R. Taha, A. El-Shafie, and M. Eslami, "Search for critical failure surface in slope stability analysis by gravitational search algorithm," *International Journal of Physical Sciences*, vol. 6, no. 21, pp. 5012–5021, 2011.

[8] M. Khajehzadeh, M. R. Taha, and M. Eslami, "Multi-objective optimisation of retaining walls using hybrid adaptive gravitational search algorithm," *Civil Engineering and Environmental Systems*, vol. 31, no. 3, pp. 229–242, 2014.

[9] Y. Abass, M. Abido, M. Al-Muhaini, and M. Khalid, "Multi-objective optimal DG sizing and placement in distribution systems using particle swarm optimization," in *2019 IEEE Innovative Smart Grid Technologies - Asia (ISGT Asia)*, pp. 1857–1861, Chengdu, China, 2019.

[10] A. Hussain, S. D. Ali Shah, and S. M. Arif, "Heuristic optimisation-based sizing and siting of DGs for enhancing resiliency of autonomous microgrid networks," *IET Smart Grid*, vol. 2, no. 2, pp. 269–282, 2019.

[11] H. Su, "Siting and sizing of distributed generators based on improved simulated annealing particle swarm optimization," *Environmental Science and Pollution Research*, vol. 26, no. 18, pp. 17927–17938, 2019.

[12] E. A. Al-Ammar, K. Farzana, A. Waqar et al., "ABC algorithm based optimal sizing and placement of DGs in distribution networks considering multiple objectives," *Ain Shams Engineering Journal*, vol. 12, no. 1, pp. 697–708, 2021.

[13] A. Ramadan, M. Ebeed, S. Kamel, E. M. Ahmed, and M. Tostado-Véliz, "Optimal allocation of renewable DGs using artificial hummingbird algorithm under uncertainty conditions," *Ain Shams Engineering Journal*, vol. 14, no. 2, article 101872, 2023.

[14] H. A. M. Pesaran, M. Nazari-Heris, B. Mohammadi-Ivatloo, and H. Seyedi, "A hybrid genetic particle swarm optimization for distributed generation allocation in power distribution networks," *Energy*, vol. 209, pp. 1–20, 2010.

[15] E. S. Ali, S. M. A. Elazim, and A. Y. Abdelaziz, "Ant lion optimization algorithm for optimal location and sizing of

renewable distributed generations," *Renewable Energy*, vol. 101, pp. 1311–1324, 2017.

[16] L. C. S. Rocha, P. R. Junior, G. Aquila, and A. Maheri, "Multi-objective optimization of hybrid wind-photovoltaic plants with battery energy storage system: current situation and possible regulatory changes," *Journal of Energy Storage*, vol. 51, article 104467, 2022.

[17] A. Ghaffari, A. Askarzadeh, and R. Fadaeinedjad, "Optimal allocation of energy storage systems, wind turbines and photovoltaic systems in distribution network considering flicker mitigation," *Applied Energy*, vol. 319, article 119253, 2022.

[18] R. S. R. K. Naidu, M. Palavalasa, and S. Chatterjee, "Integration of hybrid controller for power quality improvement in photovoltaic/wind/battery sources," *Journal of Cleaner Production*, vol. 330, pp. 129914-129915, 2022.

[19] A. Giallanza, M. Porretto, G. L. Puma, and G. Marannano, "A sizing approach for stand-alone hybrid photovoltaic-wind-battery systems: a Sicilian case study," *Journal of Cleaner Production*, vol. 199, pp. 817–830, 2018.

[20] L. M. Halabi and S. Mekhilef, "Flexible hybrid renewable energy system design for a typical remote village located in tropical climate," *Journal of Cleaner Production*, vol. 177, pp. 908–924, 2018.

[21] S. K. A. Shezan, S. Julai, M. A. Kibria et al., "Performance analysis of an off-grid wind-PV (photovoltaic)-diesel-battery hybrid energy system feasible for remote areas," *Journal of Cleaner Production*, vol. 125, pp. 121–132, 2016.

[22] A. Naderipour, H. Kamyab, J. J. Klemeš et al., "Optimal design of hybrid grid-connected photovoltaic/wind/battery sustainable energy system improving reliability, cost and emission," *Energy*, vol. 257, article 124679, 2022.

[23] A. Askarzadeh, "Distribution generation by photovoltaic and diesel generator systems: energy management and size optimization by a new approach for a stand-alone application," *Energy*, vol. 122, pp. 542–551, 2017.

[24] G. N. D. D. Doile, P. R. Junior, L. C. S. Rocha et al., "Feasibility of hybrid wind and photovoltaic distributed generation and battery energy storage systems under techno-economic regulation," *Renewable Energy*, vol. 195, pp. 1310–1323, 2022.

[25] S. Ahmadi and S. Abdi, "Application of the hybrid big bang–big crunch algorithm for optimal sizing of a stand-alone hybrid PV/wind/battery system," *Solar Energy*, vol. 134, pp. 366–374, 2016.

[26] X. M. Lin, N. Kireeva, A. V. Timoshin, A. Naderipour, Z. Abdul-Malek, and H. Kamyab, "A multi-criteria framework for designing of stand-alone and grid-connected photovoltaic, wind, battery clean energy system considering reliability and economic assessment," *Energy*, vol. 224, article 120154, 2021.

[27] M. J. Hadidian-Moghaddam, S. Arabi-Nowdeh, and M. Bigdeli, "Optimal sizing of a stand-alone hybrid photovoltaic/wind system using new grey wolf optimizer considering reliability," *Journal of Renewable and Sustainable Energy*, vol. 8, no. 3, article 035903, 2016.

[28] A. Shaqour, H. Farzaneh, Y. Yoshida, and T. Hinokuma, "Power control and simulation of a building integrated stand-alone hybrid PV-wind-battery system in Kasuga City, Japan," *Energy Reports*, vol. 6, pp. 1528–1544, 2020.

[29] C. Baglivo, D. Mazzeo, G. Oliveti, and P. M. Congedo, "Technical data of a grid-connected photovoltaic/wind hybrid system with and without storage battery for residential buildings located in a warm area," *Data in Brief*, vol. 20, pp. 587–590, 2018.

[30] B. Abu-Hijleh, "Use of hybrid PV and wind turbine–grid connected system in a local Emirati home in Dubai-UAE," *Energy Procedia*, vol. 100, pp. 463–468, 2016.

[31] H. HassanzadehFard and A. Jalilian, "Optimal sizing and location of renewable energy based DG units in distribution systems considering load growth," *International Journal of Electrical Power & Energy Systems*, vol. 101, pp. 356–370, 2018.

[32] S. Vakili, A. Schönborn, and A. I. Ölçer, "Techno-economic feasibility of photovoltaic, wind and hybrid electrification systems for stand-alone and grid-connected shipyard electrification in Italy," *Journal of Cleaner Production*, vol. 366, article 132945, 2022.

[33] A. M. Ghaithan, A. Mohammed, A. Al-Hanbali, A. M. Attia, and H. Saleh, "Multi-objective optimization of a photovoltaic-wind-grid connected system to power reverse osmosis desalination plant," *Energy*, vol. 251, article 123888, 2022.

[34] R. Fathi, B. Tousi, and S. Galvani, "A new approach for optimal allocation of photovoltaic and wind clean energy resources in distribution networks with reconfiguration considering uncertainty based on info-gap decision theory with risk aversion strategy," *Journal of Cleaner Production*, vol. 295, article 125984, 2021.

[35] A. Arasteh, P. Alemi, and M. Beiraghi, "Optimal allocation of photovoltaic/wind energy system in distribution network using meta-heuristic algorithm," *Applied Soft Computing*, vol. 109, article 107594, 2021.

[36] B. Sultana, M. W. Mustafa, U. Sultana, and A. R. Bhatti, "Review on reliability improvement and power loss reduction in distribution system via network reconfiguration," *Renewable and Sustainable Energy Reviews*, vol. 66, pp. 297–310, 2016.

[37] K. M. Jagtap and D. K. Khatod, "Novel approach for loss allocation of distribution networks with DGs," *Electric Power Systems Research*, vol. 143, pp. 303–311, 2017.

[38] M. J. Vahid-Pakdel and B. Mohammadi-ivatloo, "Probabilistic assessment of wind turbine impact on distribution networks using linearized power flow formulation," *Electric Power Systems Research*, vol. 162, pp. 109–117, 2018.

[39] A. Ali, D. Raisz, and K. Mahmoud, "Optimal oversizing of utility-owned renewable DG inverter for voltage rise prevention in MV distribution systems," *International Journal of Electrical Power & Energy Systems*, vol. 105, pp. 500–513, 2019.

[40] S. R. Gampa, K. Jasthi, P. Goli, D. Das, and R. C. Bansal, "Grasshopper optimization algorithm based two stage fuzzy multiobjective approach for optimum sizing and placement of distributed generations, shunt capacitors and electric vehicle charging stations," *Journal of Energy Storage*, vol. 27, article 101117, 2020.

[41] O. Khoubseresht and H. Shayanfar, "The role of demand response in optimal sizing and siting of distribution energy resources in distribution network with time-varying load: an analytical approach," *Electric Power Systems Research*, vol. 180, article 106100, 2020.

[42] M. Dehghani, Z. Montazeri, O. P. Malik, and O. P. Malik, "Optimal sizing and placement of capacitor banks and distributed generation in distribution systems using spring search algorithm," *International Journal of Emerging Electric Power Systems*, vol. 21, no. 1, 2020.

[43] A. Selim, S. Kamel, and F. Jurado, "Efficient optimization technique for multiple DG allocation in distribution networks," *Applied Soft Computing*, vol. 86, article 105938, 2020.

[44] C. Mokhtara, B. Negrou, N. Settou, B. Settou, and M. M. Samy, "Design optimization of off-grid hybrid renewable energy systems considering the effects of building energy performance and climate change: case study of Algeria," *Energy*, vol. 219, article 119605, 2021.

[45] A. Swarnkar, N. Gupta, and K. R. Niazi, "Adapted ant colony optimization for efficient reconfiguration of balanced and unbalanced distribution systems for loss minimization," *Swarm and Evolutionary Computation*, vol. 1, no. 3, pp. 129–137, 2011.

[46] H. R. Esmaeilian and R. Fadaeinedjad, "Optimal reconfiguration and capacitor allocation in unbalanced distribution network considering power quality issues," in *22nd International Conference and Exhibition on Electricity Distribution (CIRED 2013)*, pp. 1–4, Stockholm, 2013.

[47] S. Ghasemi, "Balanced and unbalanced distribution networks reconfiguration considering reliability indices," *Ain Shams Engineering Journal*, vol. 9, no. 4, pp. 1567–1579, 2018.

[48] A. Y. Abdelaziz, Y. G. Hegazy, W. El-Khattam, and M. M. Othman, "Optimal allocation of stochastically dependent renewable energy based distributed generators in unbalanced distribution networks," *Electric Power Systems Research*, vol. 119, pp. 34–44, 2015.

[49] A. Hadi Abdulwahid, M. Al-Razgan, H. F. Fakhruldeen et al., "Stochastic multi-objective scheduling of a hybrid system in a distribution network using a mathematical optimization algorithm considering generation and demand uncertainties," *Mathematics*, vol. 11, no. 18, p. 3962, 2023.